Appendix A.46:

113A Palmers Rd – CPT 29740

Table 1: Site Description for 113A Palmers Rd (CPT 29740).

Attribute	Yes/No			Description/Date	Symbol in Figure 1
	10-m Buffer	20-m Buffer	50-m Buffer		
Near a body of surface water or other free face features?	No	No	No	The center of the site is ~540 m to the NE from the Avon River (the free-face height is ~1.5 m) and ~1200 m to the W from the Pegasus Bay.	NA
Lateral spreading observed during the CES?	No	No	No	No lateral spreading was observed by the mapping team.[1] Only local lateral spreading for the Jun-11 EQ was observed at the property in the E portion of the 50-m buffer.	NA
Nearby buildings or structures?	Yes	Yes	Yes	Building coverage of the 10-, 20-, and 50-m buffers is 22%, 28%, and 31%, respectively. They are in all quadrants of all buffers.	White Fill + Brown Outline
Sloping land?	No	No	No	Flat land, residential area	NA
Step changes in the ground surface?	No	No	No	NA	NA
Retaining walls?	No	No	No	NA	NA
Vegetation?	Yes	Yes	Yes	Trees and bushes cover 13, 21, and 24% of the 10-, 20-, and 50-m buffers, respectively. They are in all quadrants of the buffers.	White Fill + Green Outline
Anthropogenic changes to the site between the LiDAR surveys?	Yes	Yes	Yes	Between Dec 2004 and Feb 2006: vegetation removal in the NW q. of the 50-m b. Between Feb 2006 and Mar 2009: vegetation removal in the E portion of all b., building removal in the S portions of all b., and building addition in all q. of all b. Between Sep 5, 2010, and Feb 7, 2011: building addition in the SE q. of all b. Between Dec 24, 2011, and Apr 2012: vegetation removal in the NW q. of the 50-m b. Between Jun 2012 and Jan 2013: building removal in the SE q. of all b. Between Mar 2013 and Aug 2013: building removal in the NW q. of the 20- and 50-m b. In Feb 2014, new pavement in the S portion of the 50-m b. (Lindis Ln). Between Sep 2014 and Jan 2015: building removal in the SE q. of the 50-m b. Between Jan 2015 and Jun 2015: building addition at the same property in the SE q. of the 50-m b.	Building Change: Orange Crossline/ Outline; Vegetation Removal: Green Crossline
Other important factors?	Yes	Yes	Yes	Low-motor-vehicle-volume road (Lindis Ln) occupies 4% of the 50-m buffer and stretches throughout its S portion. Veranda in the SE quadrant of all buffers.	Road: Gray Fill + Red Outline; Veranda: Purple Outline + White Fill

Note: Buffer is the area within a circle of a specified radius with CPT investigations done at its center (172.714230°, -43.500972°).

[1] Canterbury Geotechnical Database. (2012). "Observed Ground Crack Locations", Map Layer CGD0400 - 23 July 2012, retrieved July 09, 2018 from https://canterburygeotechnicaldatabase.projectorbit.com/

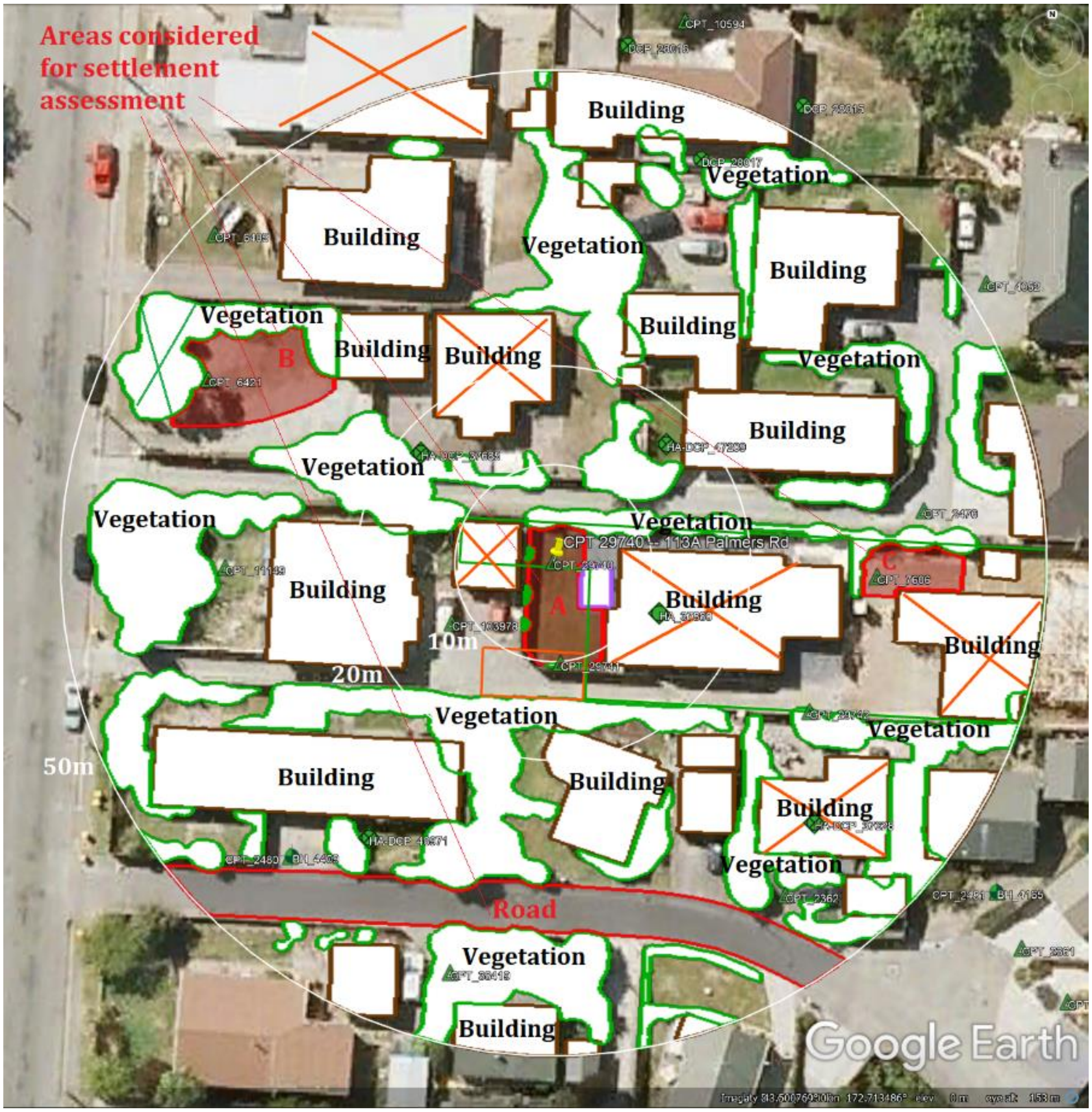

Figure 1: Site plan with areas where ejecta-induced settlement is considered.

Note 1: Patches A, B, and C (outlined in red) in the free field were selected for settlement assessment as areas free of vegetation and structures. Other important factors for the patch selection were the proximity of a patch to a CPT, a property subjected to addition and/or demolition of a structure, front yard/backyard alterations (e.g., ploughing, rubble, scrap), and aerial distribution of sediment ejecta. The entire portion of the road within the 50-m buffer was considered for settlement assessment. The LiDAR-based settlement analyses of Patch B were not performed for any earthquake event due to the evident absence of ejecta. The July 2003 LiDAR survey was not considered for the Sep-10 EQ due to the evident absence of ejecta from Patches A and C and Road (and the anthropogenic changes between the July 2003 and Sep 2010 LiDAR surveys within Patches A and C). Patch C was excluded from the settlement assessment following the June 2011 earthquake due to lateral spreading at the property, as reported by the LDAT inspection team. The Oct 2015 LiDAR survey was not considered for the Road.

Table 2: LiDAR flight error adjustments, global adjustments for the difference between average LiDAR point elevations and benchmark survey elevations, and vertical tectonic movement adjustments.

	Adjustments (mm)		
Earthquake Event(s)	LiDAR Flight Error	Global Offset[2]	Tectonic Vertical Movement
Sep-10	0	-3	0
Feb-11	0	16	-25
Jun-11	0	38	-50
Dec-11	-50	-65	+15
CES	-50	-14	-60
Any LiDAR survey affected by ejecta?			Yes*

Note: The negative sign indicates the subtraction from the ground surface subsidence, while the positive sign indicates the addition to the ground surface subsidence; * It is likely that ejecta were not removed from Patch C and Road (as per the satellite image from 8 Mar 2011), which requires the addition of ~100 mm to the ground surface subsidence for the Feb-11 EQ and the subtraction of ~100 mm from the ground surface subsidence for the Jun-11 EQ.

Table 3a: LiDAR Measurement Error for Patch A.

Surveys	Buffer	Area Averaged Difference Indicating Repeat Measurement Error (mm)	$\sigma^*_{\text{individual LiDAR points}}$ (mm)	%Reduction in σ due to Area Averaging of LiDAR Points
Post Feb 2011: Mar 2011 and May 2011	10-m	79	59	[134,134]
	20-m	79		
	50-m	79		
Post Dec 2011: Feb 2012 and Oct 2015	10-m	49	70	[70,70]
	20-m	49		
	50-m	49		

*Standard deviation.

[2] Russell, J., & van Ballegooy, S. (2015). *Canterbury Earthquake Sequence: Increased liquefaction vulnerability assessment methodology*. New Zealand: Tonkin & Taylor Ltd.

Table 3b: LiDAR Measurement Error for Patch B.

Surveys	Buffer	Area Averaged Difference Indicating Repeat Measurement Error (mm)	ϭ*individual LiDAR points (mm)	%Reduction in ϭ due to Area Averaging of LiDAR Points
Post Feb 2011: Mar 2011 and May 2011	10-m	NA	59	[ND,ND]
	20-m	NA		
	50-m	ND		
Post Dec 2011: Feb 2012 and Oct 2015	10-m	NA	70	[ND,ND]
	20-m	NA		
	50-m	ND		

*Standard deviation; NA = Not available; ND = Not determined.

Table 3c: LiDAR Measurement Error for Patch C.

Surveys	Buffer	Area Averaged Difference Indicating Repeat Measurement Error (mm)	ϭ*individual LiDAR points (mm)	%Reduction in ϭ due to Area Averaging of LiDAR Points
Post Feb 2011: Mar 2011 and May 2011	10-m	NA	59	[117,117]
	20-m	NA		
	50-m	69		
Post Dec 2011: Feb 2012 and Oct 2015	10-m	NA	70	[ND,ND]
	20-m	NA		
	50-m	ND		

*Standard deviation; NA = Not available; ND = Not determined.

Table 3d: LiDAR Measurement Error for Road.

Surveys	Buffer	Area Averaged Difference Indicating Repeat Measurement Error (mm)	$\sigma^*_{\text{individual LiDAR points}}$ (mm)	%Reduction in σ due to Area Averaging of LiDAR Points
Post Feb 2011: Mar 2011 and May 2011	10-m	NA	59	[127,127]
	20-m	NA		
	50-m	75		
Post Dec 2011: Feb 2012 and Oct 2015	10-m	NA	70	[ND,ND]
	20-m	NA		
	50-m	ND		

*Standard deviation; ND = Not determined.

Table 4a: Ground surface subsidence adjustments due to LiDAR measurement error for Patch A.

Earthquake Event(s)	$\sigma_{\text{pre-EQ LiDAR survey}}$ (mm)	$\sigma_{\text{post-EQ LiDAR survey}}$ (mm)	σ_{total} (mm)	Area Average Adjusted σ (mm) **
Sep-10	158	56	134	$\pm$180
Feb-11	56	59	59	$\pm$79
Jun-11	59	61	62	$\pm$83
Dec-11	61	70	87	$\pm$116
CES	158	70	124	$\pm$167

**Based on the highest %Reduction in Table 3a.

Table 4b: Ground surface subsidence adjustments due to LiDAR measurement error for Patch B.

Earthquake Event(s)	$\sigma_{\text{pre-EQ LiDAR survey}}$ (mm)	$\sigma_{\text{post-EQ LiDAR survey}}$ (mm)	σ_{total} (mm)	Area Average Adjusted σ (mm) **
Sep-10	158	56	134	ND
Feb-11	56	59	59	ND
Jun-11	59	61	62	ND
Dec-11	61	70	87	ND
CES	158	70	124	ND

**Based on the highest %Reduction in Table 3b.

Table 4c: Ground surface subsidence adjustments due to LiDAR measurement error for Patch C.

Earthquake Event(s)	$\sigma_{\text{pre-EQ LiDAR survey}}$ (mm)	$\sigma_{\text{post-EQ LiDAR survey}}$ (mm)	σ_{total} (mm)	Area Average Adjusted σ (mm) **
Sep-10	158	56	134	±157
Feb-11	56	59	59	±69
Jun-11	59	61	62	±73
Dec-11	61	70	87	±101
CES	158	70	124	±146

**Based on the highest %Reduction in Table 3c.

Table 4d: Ground surface subsidence adjustments due to LiDAR measurement error for Road.

Earthquake Event(s)	$\sigma_{\text{pre-EQ LiDAR survey}}$ (mm)	$\sigma_{\text{post-EQ LiDAR survey}}$ (mm)	σ_{total} (mm)	Area Average Adjusted σ (mm) **
Sep-10	158	56	134	±170
Feb-11	56	59	59	±75
Jun-11	59	61	62	±79
Dec-11	61	70	87	±110
CES	158	70	124	±158

**Based on the highest %Reduction in Table 3d.

Table 5a: Raw liquefaction-related ground surface subsidence using original LiDAR points for Patch A.

	Average Ground Surface Subsidence (mm)		
Earthquake Event(s)	10-m Buffer	20-m Buffer	50-m Buffer
Sep-10	ND	ND	ND
Feb-11	205	205	205
Jun-11	142	142	142
Dec-11	111	111	111
CES	ND	ND	ND

ND = Not determined.

Table 5b: Raw liquefaction-related ground surface subsidence using original LiDAR points for Patch B.

Earthquake Event(s)	Average Ground Surface Subsidence (mm)		
	10-m Buffer	20-m Buffer	50-m Buffer
Sep-10	NA	NA	ND
Feb-11	NA	NA	ND
Jun-11	NA	NA	ND
Dec-11	NA	NA	ND
CES	NA	NA	ND

NA = Not available; ND = Not determined.

Table 5c: Raw liquefaction-related ground surface subsidence using original LiDAR points for Patch C.

Earthquake Event(s)	Average Ground Surface Subsidence (mm)		
	10-m Buffer	20-m Buffer	50-m Buffer
Sep-10	NA	NA	ND
Feb-11	NA	NA	-50
Jun-11	NA	NA	ND
Dec-11	NA	NA	ND
CES	NA	NA	ND

NA = Not available; ND = Not determined.

Table 5d: Raw liquefaction-related ground surface subsidence using original LiDAR points for Road.

Earthquake Event(s)	Average Ground Surface Subsidence (mm)		
	10-m Buffer	20-m Buffer	50-m Buffer
Sep-10	NA	NA	ND
Feb-11	NA	NA	57
Jun-11	NA	NA	139
Dec-11	NA	NA	117
CES	NA	NA	ND

NA = Not available; ND = Not determined.

Table 6a: Corrected liquefaction-related ground surface subsidence using original LiDAR points for Patch A with the calculated adjustments in Table 2.

Earthquake Event(s)	Average Calculated Ground Surface Subsidence (mm)		
	10-m Buffer	20-m Buffer	50-m Buffer
Sep-10	ND	ND	ND
Feb-11	196±75	196±75	196±75
Jun-11	130±75	130±75	130±75
Dec-11	11±125	11±125	11±125
CES	ND	ND	ND

Notes: Plus/minus values are same as those in Table 4a, but rounded to the nearest 25 mm; Positive overall values indicate ground surface subsidence, while negative overall values indicate ground surface uplift; ND = Not determined.

Table 6b: Corrected liquefaction-related ground surface subsidence using original LiDAR points for Patch B with the calculated adjustments in Table 2.

Earthquake Event(s)	Average Calculated Ground Surface Subsidence (mm)		
	10-m Buffer	20-m Buffer	50-m Buffer
Sep-10	NA	NA	ND
Feb-11	NA	NA	ND
Jun-11	NA	NA	ND
Dec-11	NA	NA	ND
CES	NA	NA	ND

Notes: Plus/minus values are same as those in Table 4b, but rounded to the nearest 25 mm; Positive overall values indicate ground surface subsidence, while negative overall values indicate ground surface uplift; ND = Not determined.

Table 6c: Corrected liquefaction-related ground surface subsidence using original LiDAR points for Patch C with the calculated adjustments in Table 2.

Earthquake Event(s)	Average Calculated Ground Surface Subsidence (mm)		
	10-m Buffer	20-m Buffer	50-m Buffer
Sep-10	NA	NA	ND
Feb-11	NA	NA	41±75
Jun-11	NA	NA	ND
Dec-11	NA	NA	ND
CES	NA	NA	ND

Notes: Plus/minus values are same as those in Table 4b, but rounded to the nearest 25 mm; Positive overall values indicate ground surface subsidence, while negative overall values indicate ground surface uplift; ND = Not determined.

Table 6d: Corrected liquefaction-related ground surface subsidence using original LiDAR points for Road with the calculated adjustments in Table 2.

Earthquake Event(s)	Average Calculated Ground Surface Subsidence (mm) 10-m Buffer	20-m Buffer	50-m Buffer
Sep-10	NA	NA	ND
Feb-11	NA	NA	148±75
Jun-11	NA	NA	26±75
Dec-11	NA	NA	17±100
CES	NA	NA	ND

Notes: Plus/minus values are same as those in Table 4a, but rounded to the nearest 25 mm; Positive overall values indicate ground surface subsidence, while negative overall values indicate ground surface uplift; ND = Not determined.

Table 7a: Corrected liquefaction-related ground surface subsidence for Patch A using LiDAR DEMs.

	Estimated Ground Surface Subsidence (mm)								
	10-m Buffer			20-m Buffer			50-m Buffer		
Earthquake Event(s)	16th %ile	50th %ile	84th %ile	16th %ile	50th %ile	84th %ile	16th %ile	50th %ile	84th %ile
Sep-10	ND	ND	ND	ND	ND	ND	ND	ND	ND
Feb-11	150	200	250	150	200	250	150	200	250
Jun-11	50	100	150	50	100	150	50	100	150
Dec-11	50	50	50	50	50	50	50	50	50
CES	ND	ND	ND	ND	ND	ND	ND	ND	ND

Note: These percentiles are not the exact statistical measures; they indicate the spatial variability of ground surface subsidence; ND = Not determined due to the anthropogenic changes.

Table 7b: Corrected liquefaction-related ground surface subsidence for Patch B using LiDAR DEMs.

	Estimated Ground Surface Subsidence (mm)								
	10-m Buffer			20-m Buffer			50-m Buffer		
Earthquake Event(s)	16th %ile	50th %ile	84th %ile	16th %ile	50th %ile	84th %ile	16th %ile	50th %ile	84th %ile
Sep-10	NA	NA	NA	NA	NA	NA	ND	ND	ND
Feb-11	NA	NA	NA	NA	NA	NA	100	100	150
Jun-11	NA	NA	NA	NA	NA	NA	<50	<50	50
Dec-11	NA	NA	NA	NA	NA	NA	100	100	100
CES	NA	NA	NA	NA	NA	NA	ND	ND	ND

Note: These percentiles are not the exact statistical measures; they indicate the spatial variability of ground surface subsidence; ND = Not determined due to the anthropogenic changes.

Table 7c: Corrected liquefaction-related ground surface subsidence for Patch C using LiDAR DEMs.

	Estimated Ground Surface Subsidence (mm)								
	10-m Buffer			20-m Buffer			50-m Buffer		
Earthquake Event(s)	16th %ile	50th %ile	84th %ile	16th %ile	50th %ile	84th %ile	16th %ile	50th %ile	84th %ile
Sep-10	NA	NA	NA	NA	NA	NA	ND	ND	ND
Feb-11	NA	NA	NA	NA	NA	NA	150	200	200
Jun-11	NA	NA	NA	NA	NA	NA	ND	ND	ND
Dec-11	NA	NA	NA	NA	NA	NA	ND	ND	ND
CES	NA	NA	NA	NA	NA	NA	ND	ND	ND

Note: These percentiles are not the exact statistical measures; they indicate the spatial variability of ground surface subsidence; ND = Not determined due to the anthropogenic changes/lateral spreading.

Table 7d: Corrected liquefaction-related ground surface subsidence for Road using LiDAR DEMs.

	Estimated Ground Surface Subsidence (mm)								
	10-m Buffer			20-m Buffer			50-m Buffer		
Earthquake Event(s)	16th %ile	50th %ile	84th %ile	16th %ile	50th %ile	84th %ile	16th %ile	50th %ile	84th %ile
Sep-10	NA	NA	NA	NA	NA	NA	50	100	100
Feb-11	NA	NA	NA	NA	NA	NA	150	150	200
Jun-11	NA	NA	NA	NA	NA	NA	<50	<50	<50
Dec-11	NA	NA	NA	NA	NA	NA	50	100	100
CES	NA	NA	NA	NA	NA	NA	300	400	450

Note: These percentiles are not the exact statistical measures; they indicate the spatial variability of ground surface subsidence.

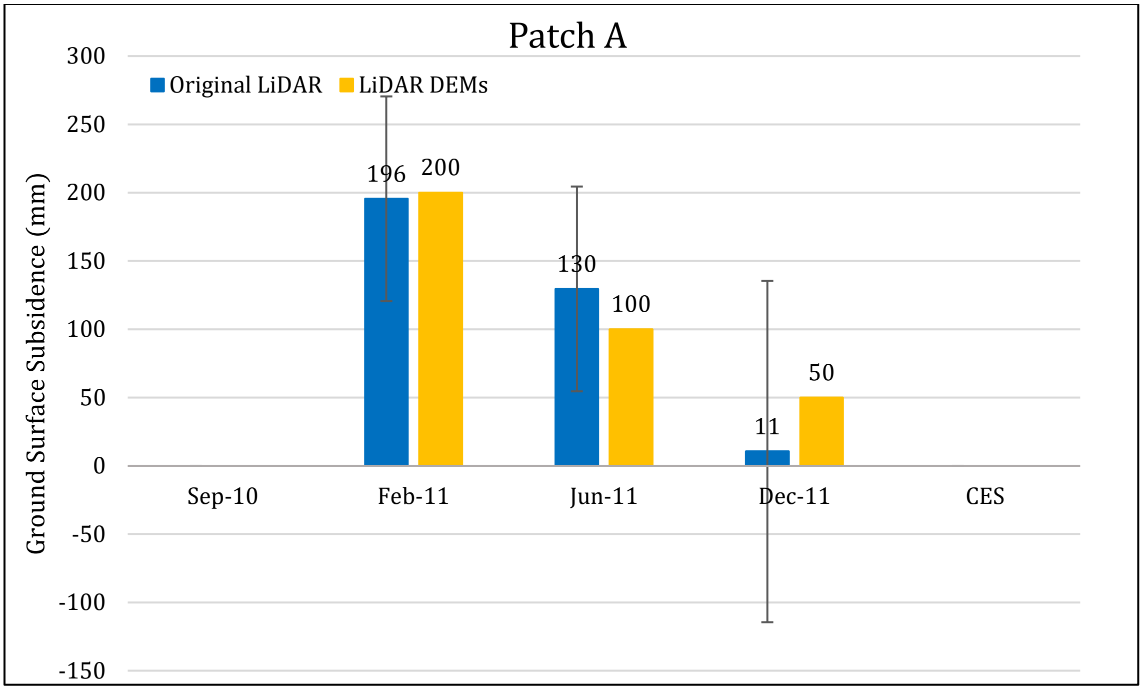

Figure 2: Comparison between ground surface subsidence determined from original LiDAR survey points and ground surface subsidence (50th %ile) estimated using LiDAR DEMs for Patch A (10-, 20-, and 50-m buffers).

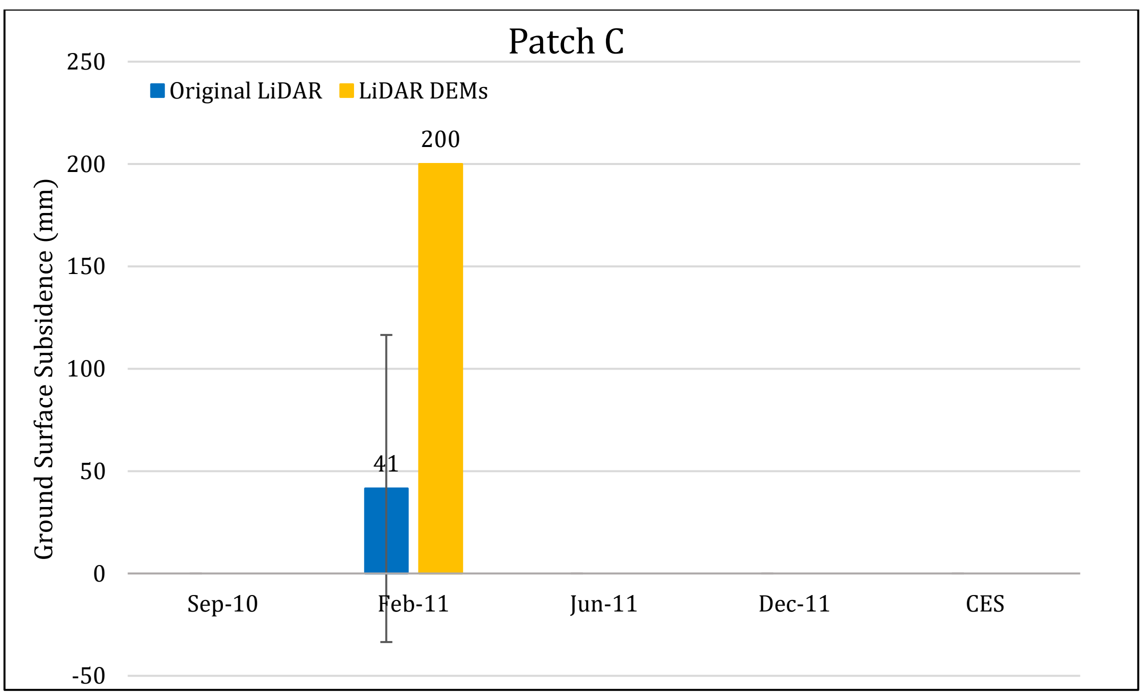

Figure 3: Comparison between ground surface subsidence determined from original LiDAR survey points and ground surface subsidence (50th %ile) estimated using LiDAR DEMs for Patch C (50-m buffer).

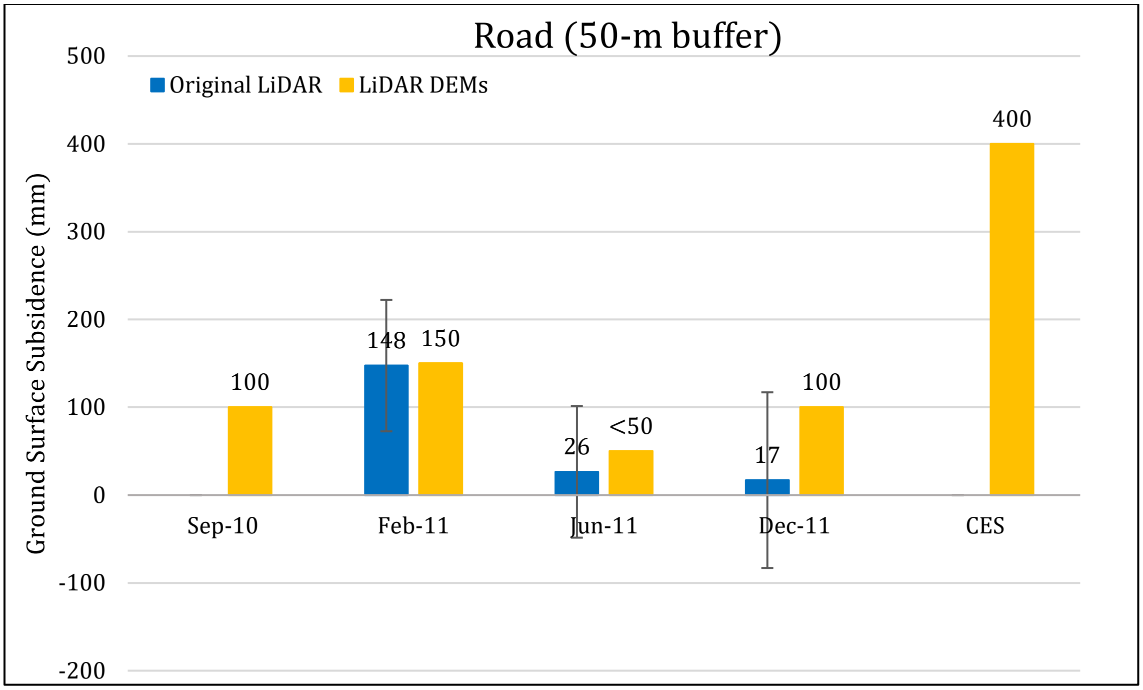

Figure 4: Comparison between ground surface subsidence determined from original LiDAR survey points and ground surface subsidence (50th %ile) estimated using LiDAR DEMs for Road (50-m buffer).

Note 2: The ground surface subsidence values determined from the original LiDAR survey points are generally consistent with the ground surface subsidence values estimated using the LiDAR DEMs. The exception to this trend occurs for Patch A for the Feb-11 earthquake as the estimated ground surface subsidence using the original LiDAR survey points is 41 mm compared to the subsidence of 200 mm estimated using the LiDAR DEMs. One of the possible explanations for this discrepancy is the DEM cell extrapolation and the lack of ground-classified points within Patch C used to develop the DEM.

Table 8a: Ejecta-Induced settlement for the top 20 m of the soil profile for Patch A for the 50th %ile PGA, P_L=50%, and C_{FC}=0.13 using BI-2014, ZRB-2002, and I_C cutoff of 2.6.

Earthquake Event(s)	M_W	PGA (g)	Depth to Groundwater (m)	S_T (mm)	S_{V1D} (mm)	$S_{E,L}$ (mm)
Sep-10	7.1	0.18	1.5	ND	16±20	ND
Feb-11	6.2	0.48	1.5	196±75	101±50	95±90
Jun-11	6.2	0.24	1.3	130±75	27±25	103±79
Dec-11	6.1	0.36	1.2	11±125	70±50	-59±135

Notes: S_T = Total settlement (Table 6); S_{V1D} = Average vertical settlement due to volumetric compression using Boulanger and Idriss (2014) (BI-2014), Zhang et al. (2002) (ZRB-2002) procedures and de Greef and Lengkeek (2018) thin-layer correction; $S_{E,L}$ = Ejecta-induced settlement as the difference between the LiDAR-based S_T and S_{V1D}; ND = Not determined.

Table 8b: Ejecta-Induced settlement for the top 20 m of the soil profile for Patch B for the 50th %ile PGA, P_L=50%, and C_{FC}=0.13 using BI-2014, ZRB-2002, and I_C cutoff of 2.6.

Earthquake Event(s)	M_W	PGA (g)	Depth to Groundwater (m)	S_T (mm)	S_{V1D} (mm)	$S_{E,L}$ (mm)
Sep-10	7.1	0.18	1.5	ND	3±20	ND
Feb-11	6.2	0.48	1.5	ND	94±50	ND
Jun-11	6.2	0.24	1.3	ND	9±25	ND
Dec-11	6.1	0.36	1.2	ND	47±50	ND

Notes: S_T = Total settlement (Table 6); S_{V1D} = Average vertical settlement due to volumetric compression using Boulanger and Idriss (2014) (BI-2014), Zhang et al. (2002) (ZRB-2002) procedures and de Greef and Lengkeek (2018) thin-layer correction; $S_{E,L}$ = Ejecta-induced settlement as the difference between the LiDAR-based S_T and S_{V1D}; ND = Not determined.

Table 8c: Ejecta-Induced settlement for the top 20 m of the soil profile for Patch C for the 50th %ile PGA, P_L=50%, and C_{FC}=0.13 using BI-2014, ZRB-2002, and I_C cutoff of 2.6.

Earthquake Event(s)	M_W	PGA (g)	Depth to Groundwater (m)	S_T (mm)	S_{V1D} (mm)	$S_{E,L}$ (mm)
Sep-10	7.1	0.18	1.5	ND	6±20	ND
Feb-11	6.2	0.48	1.5	41±75	59±50	-18±90
Jun-11	6.2	0.24	1.3	ND	14±25	ND
Dec-11	6.1	0.36	1.2	ND	43±50	ND

Notes: S_T = Total settlement (Table 6); S_{V1D} = Average vertical settlement due to volumetric compression using Boulanger and Idriss (2014) (BI-2014), Zhang et al. (2002) (ZRB-2002) procedures and de Greef and Lengkeek (2018) thin-layer correction; $S_{E,L}$ = Ejecta-induced settlement as the difference between the LiDAR-based S_T and S_{V1D}; ND = Not determined.

Table 8d: Ejecta-Induced settlement for the top 20 m of the soil profile for Road for the 50th %ile PGA, P_L=50%, and C_{FC}=0.13 using BI-2014, ZRB-2002, and I_C cutoff of 2.6.

Earthquake Event(s)	M_W	PGA (g)	Depth to Groundwater (m)	S_T (mm)	S_{V1D} (mm)	$S_{E,L}$ (mm)
Sep-10	7.1	0.18	1.5	ND	27±20	ND
Feb-11	6.2	0.48	1.5	148±75	125±50	23±90
Jun-11	6.2	0.24	1.3	26±75	46±25	-20±79
Dec-11	6.1	0.36	1.2	17±100	90±50	-73±112

Notes: S_T = Total settlement (Table 6); S_{V1D} = Average vertical settlement due to volumetric compression using Boulanger and Idriss (2014) (BI-2014), Zhang et al. (2002) (ZRB-2002) procedures and de Greef and Lengkeek (2018) thin-layer correction; $S_{E,L}$ = Ejecta-induced settlement as the difference between the LiDAR-based S_T and S_{V1D}; ND = Not determined.

Note 3: The uncertainty for volumetric settlement was derived based on the sensitivity of volumetric settlement to PGA, C_{FC}, and P_L for each earthquake event for VsVp 57203 *Shirley Intermediate School* and CC LIQ 1 – CPT 5586 – *Vivian St* sites. Taking the 50th percentile as the baseline case, the minimum and maximum values corresponding to the difference between the 25th percentile and the 50th percentile and the 75th percentile and the 50th percentile were determined. The arithmetic mean of the range of the minimum and maximum difference was evaluated for each patch at the two sites. The maximum arithmetic mean for each earthquake event was rounded to the nearest five and used as the uncertainty value. Accordingly, the 1-D volumetric settlement uncertainties of ±20, ±50, ±25, and ±50 mm for the Sep-10, Feb-11, Jun-11, and Dec-11 earthquake events, respectively, were used for all sites in this study.

Table 9a: Coverage area and height of ejecta estimates for Patch A using photographs.

EQ Event	$H_{E,thick1}$ (mm)	$A_{E,thick1}$ (m^2)	$H_{E,thick2}$ (mm)	$A_{E,thick2}$ (m^2)	$H_{E,thin1}$ (mm)	$A_{E,thin1}$ (m^2)	$H_{E,thin2}$ (mm)	$A_{E,thin2}$ (m^2)	A_T (m^2)
Sep-10	0	0	0	0	0	0	0	0	82.4
Feb-11	150-250	11.5	100-150	14.5	50-70	12.2	5-10	39.9	82.4
Jun-11	0	0	40-80	51.8	0	0	5-10	30.6	82.4
Dec-11	80-160	26.6	40-80	23.0	30-60	9.8	5-10	23.0	82.4

Notes: $A_{E,thick/thin}$ = Coverage area of thick/thin ejecta layers; $H_{E,thick/thin}$ = Lower-upper estimate of height of thick/thin ejecta layers; A_T = Total assessment area of a buffer being considered; Thin and thick layers correspond to light gray and dark gray colors of ejecta observed in aerial photographs.

Table 9b: Coverage area and height of ejecta estimates for Patch B using photographs.

Earthquake Event	$A_{E,thick}$ (m^2)	$H_{E,thick}$ (mm)	$A_{E,thin}$ (m^2)	$H_{E,thin}$ (mm)	A_T (m^2)
Sep-10	0	0	0	0	112
Feb-11	0	0	0	0	112
Jun-11	0	0	0	0	112
Dec-11	0	0	0	0	112

Notes: $A_{E,thick/thin}$ = Coverage area of thick/thin ejecta layers; $H_{E,thick/thin}$ = Lower-upper estimate of height of thick/thin ejecta layers; A_T = Total assessment area of a buffer being considered; Thin and thick layers correspond to light gray and dark gray colors of ejecta observed in aerial photographs.

Table 9c: Coverage area and height of ejecta estimates for Patch C using photographs.

Earthquake Event	$A_{E,thick1}$ (m²)	$H_{E,thick1}$ (mm)	$A_{E,thick2}$ (m²)	$H_{E,thick2}$ (mm)	$A_{E,thin1}$ (m²)	$H_{E,thin1}$ (mm)	A_T (m²)
Sep-10	0	0	0	0	0	0	36.2
Feb-11	10.5	200-300	5.7	40-60	6.4	10-20	36.2
Jun-11	ND	ND	ND	ND	ND	ND	36.2
Dec-11	ND	ND	ND	ND	ND	ND	36.2

Notes: $A_{E,thick/thin}$ = Coverage area of thick/thin ejecta layers; $H_{E,thick/thin}$ = Lower-upper estimate of height of thick/thin ejecta layers; A_T = Total assessment area of a buffer being considered; Thin and thick layers correspond to light gray and dark gray colors of ejecta observed in aerial photographs; ND = Not determined due to the lateral spreading.

Table 9d: Coverage area and height of ejecta estimates for Road using photographs.

EQ Event	$H_{E,thick1}$ (mm)	$A_{E,thick1}$ (m²)	$H_{E,thick2}$ (mm)	$A_{E,thick2}$ (m²)	$H_{E,thin1}$ (mm)	$A_{E,thin1}$ (m²)	$H_{E,thin2}$ (mm)	$A_{E,thin2}$ (m²)	A_T (m²)
Sep-10	0	0	0	0	0	0	0	0	296
Feb-11	120-250	149	80-120	28.0	30-60	115	20-40	4.3	296
Jun-11	0	0	40-100	290	20-40	5.9	0	0	296
Dec-11	80-160	24.9	60-120	167	30-60	72.0	2-4	25.5	289*

Notes: $A_{E,thin/thick}$ = Coverage area of thin/thick ejecta layers; $H_{E,thin/thick}$ = Lower-upper estimate of height of thin/thick ejecta layers; Thin and thick layers correspond to light gray and dark gray colors of ejecta observed in aerial photographs; A_T= Total assessment area of a buffer being considered; * indicates reduction in A_T due to the presence of objects.

Note 4: The values in Table 9 correspond to the coverage area of ejecta outlined in aerial photographs (Figures 27, 29, and 68-70) and the lower and upper estimates of ejecta height based on geometrical approximations, ground photographs (Figures 72, 74, 76, 78, and 79), and EQC LDAT property inspection reports (e.g., Figures 71, 73, 75, and 77). The ejecta-induced settlement using photographs and engineering judgment, $S_{E,P}$, is estimated as

$$S_{E,P} = \frac{\sum_{i=1}^{a} A_{E,thick,i} * H_{E,thick,i} + \sum_{j=1}^{b} A_{E,thin,j} * H_{E,thin,j}}{A_T} = \frac{\sum_{i=1}^{a} V_{E,thick,i} + \sum_{j=1}^{b} V_{E,thin,j}}{A_T}$$

where

- $A_{E,thick,i}$ and $H_{E,thick,i}$ are the area and the height, respectively, of a thick ejecta layer;
- $A_{E,thin,j}$ and $H_{E,thin,j}$ are the area and the height, respectively, of a thin ejecta layer;
- A_T is the total assessment area for a buffer being considered (Figure 1).

Table 10a: Ejecta-induced settlement estimates for Patches A, B, and C based on photographs.

Earthquake Event	Patch A		Patch B		Patch C	
	$S_{E,P,lower}$ (mm)	$S_{E,P,upper}$ (mm)	$S_{E,P,lower}$ (mm)	$S_{E,P,upper}$ (mm)	$S_{E,P,lower}$ (mm)	$S_{E,P,upper}$ (mm)
Sep-10	0	0	0	0	0	0
Feb-11	48	77	0	0	65	98
Jun-11	27	54	0	0	ND	ND
Dec-11	42	84	0	0	ND	ND

Note: $S_{E,P,lower}$ and $S_{E,P,upper}$ correspond to lower and upper estimates of $S_{E,P}$, respectively; ND = Not determined due to lateral spreading.

Table 10b: Ejecta-induced settlement estimates for Road based on photographs.

Earthquake Event	Road	
	$S_{E,P,lower}$ (mm)	$S_{E,P,upper}$ (mm)
Sep-10	0	0
Feb-11	80	161
Jun-11	40	99
Dec-11	49	98

Note: $S_{E,P,lower}$ and $S_{E,P,upper}$ correspond to lower and upper estimates of $S_{E,P}$, respectively.

Table 11a: Best final estimates of ejecta-induced settlement for Patches A, B, and C.

EQ Event	Patch A			Patch B			Patch C		
	$S_{E,L}$ (mm)	$S_{E,P}$ (mm)	$S_{E,final}$ (mm)	$S_{E,L}$ (mm)	$S_{E,P}$ (mm)	$S_{E,final}$ (mm)	$S_{E,L}$ (mm)	$S_{E,P}$ (mm)	$S_{E,final}$ (mm)
Sep-10	ND	0	0	ND	0	0	ND	0	0
Feb-11	95±90	63±14	80±45	ND	0	0	-18±90	82±16	80±15
Jun-11	103±79	41±13	70±40	ND	0	0	ND	ND	ND
Dec-11	-59±135	63±21	65±20	ND	0	0	ND	ND	ND

Notes: $S_{E,L}$ = Ejecta-induced settlement based on LiDAR data reported in Table 8; $S_{E,P}$ = Median ejecta-induced settlement for the range of values reported in Table 10; $S_{E,final}$ = Best final estimate of ejecta-induced settlement rounded to the nearest 5 mm; Final plus/minus values are also rounded to the nearest 5 mm; ND = Not determined due to anthropogenic changes/lateral spreading/absence of ejecta.

Table 11b: Best final estimates of ejecta-induced settlement for Road.

Earthquake Event	Road (50-m buffer)		
	$S_{E,L}$ (mm)	$S_{E,P}$ (mm)	$S_{E,final}$ (mm)
Sep-10	ND	0	0
Feb-11	23±90	121±40	120±40
Jun-11	-20±79	70±29	70±30
Dec-11	-73±112	74±24	75±25

Notes: $S_{E,L}$ = Ejecta-induced settlement based on LiDAR data reported in Table 8; $S_{E,P}$ = Median ejecta-induced settlement for the range of values reported in Table 10; $S_{E,final}$ = Best final estimate of ejecta-induced settlement rounded to the nearest 5 mm; Final plus/minus values are also rounded to the nearest 5 mm; ND = Not determined due to absence of ejecta.

Note 5:

- Patch A: $S_{E,final}$ for the Sep-10 and Dec-11 EQs is based solely on $S_{E,P}$ due to the evident absence of ejecta for the Sep-10 EQ and the negative $S_{E,L}$ values for the Dec-11 EQ. $S_{E,final}$ for the Feb-11 and Jun-11 EQs is the weighted average of $S_{E,L}$ and $S_{E,P}$ with weights of 1/2 and 1/2, respectively. The uncertainty associated with $S_{E,final}$ is also the weighted average of uncertainties associated with $S_{E,L}$ and $S_{E,P}$ with the same respective weights of 1/2 and 1/2.
- Patch B: $S_{E,final}$ is based solely on $S_{E,P}$ for all earthquake events due to the evident absence of ejecta.
- Patch C: $S_{E,final}$ for the Sep-10 and Feb-11 EQs is based solely on $S_{E,P}$ due to the evident absence of ejecta for the Sep-10 EQ and the negative $S_{E,L}$ value for the Feb-11 EQ. $S_{E,final}$ for the Jun-11 and Dec-11 EQs was not determined due to lateral spreading. (As a side note, there are shadows in the Jun-11 aerial photographs and vegetation in the Dec-11 aerial photograph, as well as the uncertainty associated with the ejecta removal at the time of the Sep-11 and Feb-12 LiDAR surveys. The house was unoccupied in July 2011.)
- Road: $S_{E,final}$ for all earthquake events is based solely on $S_{E,P}$ due to the evident absence of ejecta for the Sep-10 EQ, the negative $S_{E,L}$ values for the Jun-11 and Dec-11 EQs, and discrepancy between physical evidence and $S_{E,L}$ for the Feb-11 EQ (see the Table 1 note).
- The weight coefficients are based on the LiDAR error bands, LPI prediction error (Maurer et al. 2014[3]), presence of ejecta at the time of LiDAR surveys, density of July 2003 LiDAR points, and completeness of visual evidence (i.e., ground and aerial photographs and EQC LDAT property inspection reports for the site). The 113A Palmers Rd site is not in the apparent zone of higher or lower ground surface subsidence for the Sep-10 and Feb-11 EQ. The site is in the zone of accurate LPI prediction of liquefaction severity for the Sep-10 and Feb-11 EQs. The LDAT inspection reports and ground photographs are available for the properties with Patches A, B, and C. The ejecta heigh was not measured for Patch A because the ejecta were almost completely removed at the time of the inspection (31 May 2011). Ejecta were not observed for Patch B. The height of ejecta at the property with Patch C was measured as 300-

[3] Maurer, B. W., Green, R. A., Cubrinovski, M., & Bradley, B. A. (2014). Evaluation of the Liquefaction Potential Index for Assessing Liquefaction Hazard in Christchurch, New Zealand. *Journal of Geotechnical and Geoenvironmental Engineering*, 140(7), 04014032-1-11. doi:10.1061/(asce)gt.1943-5606.0001117

400 mm (31 May 2011). Following the Jun-11 EQ, there were 200-300 mm of ejecta in height across the entire property and lateral spreading occurred; thus, Patch C was not assessed for ejecta-induced settlement for the Jun-11 and Dec-11 EQs. The ejecta height typically ranged from 100 mm to 350 mm at the properties within the 50-m buffer; at some places the ejecta height even reached 500 mm. There are no ground photographs of ejecta on the road.

- The $S_{E,L}$ values for the road differ significantly from the $S_{E,P}$ values for the road. The significant discrepancy between the two sets of values might be due to the shear displacement driven by gently sloping land from the properties toward the road, which could have pushed the road up; this mechanism could not be captured by LiDAR and 1-D volumetric settlement.

Summary:

- **The best estimate of the ejecta-induced free-field ground settlement at the 113A Palmers Rd site for the SEP 2010, FEB 2011, JUN 2011, and DEC 2011 earthquake is 0 mm, 80±45 mm, 70±40 mm, and 65±20 mm, respectively.**
- **The best estimate of the ejecta-induced free-field ground settlement of the road at the 113A Palmers Rd site for the SEP 2010, FEB 2011, JUN 2011, and DEC 2011 earthquake is 0 mm, 120±40 mm, 70±30 mm, and 75±25 mm, respectively.**

Figure 5: Location of the site.

Figure 6: Position of the site relative to nearby buildings, vegetation, and free-face features.

Figure 7: Street view of the flat land.

Figure 8: Satellite image of the site taken in Dec 2004.

Figure 9: Satellite image of the site taken in Feb 2006.

Figure 10: Satellite image of the site taken in Mar 2009.

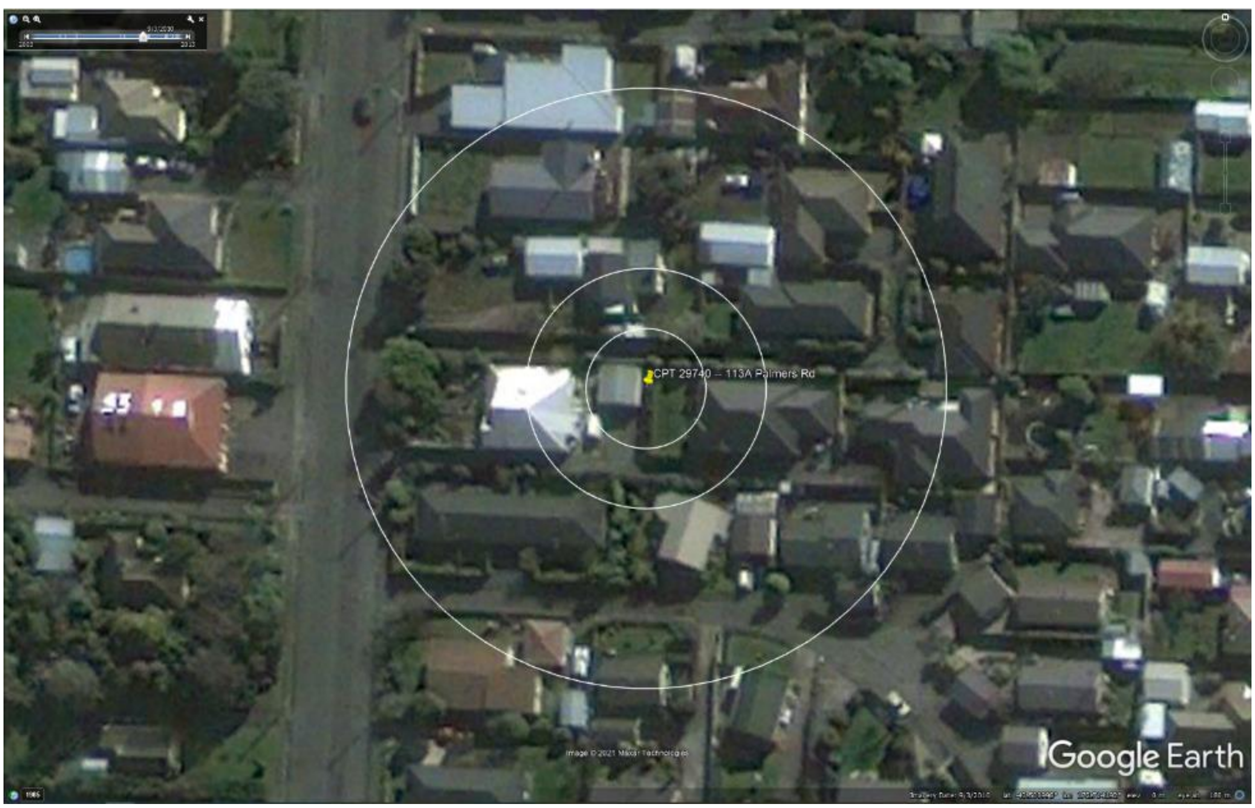

Figure 11: Satellite image of the site taken on Sep 3, 2010.

Figure 12: Satellite image of the site taken on Sep 5, 2010.

Figure 13: Satellite image of the site taken on Feb 7, 2011.

Figure 14: Satellite image of the site taken on Feb 23, 2011.

Figure 15: Satellite image of the site taken on Feb 26, 2011.

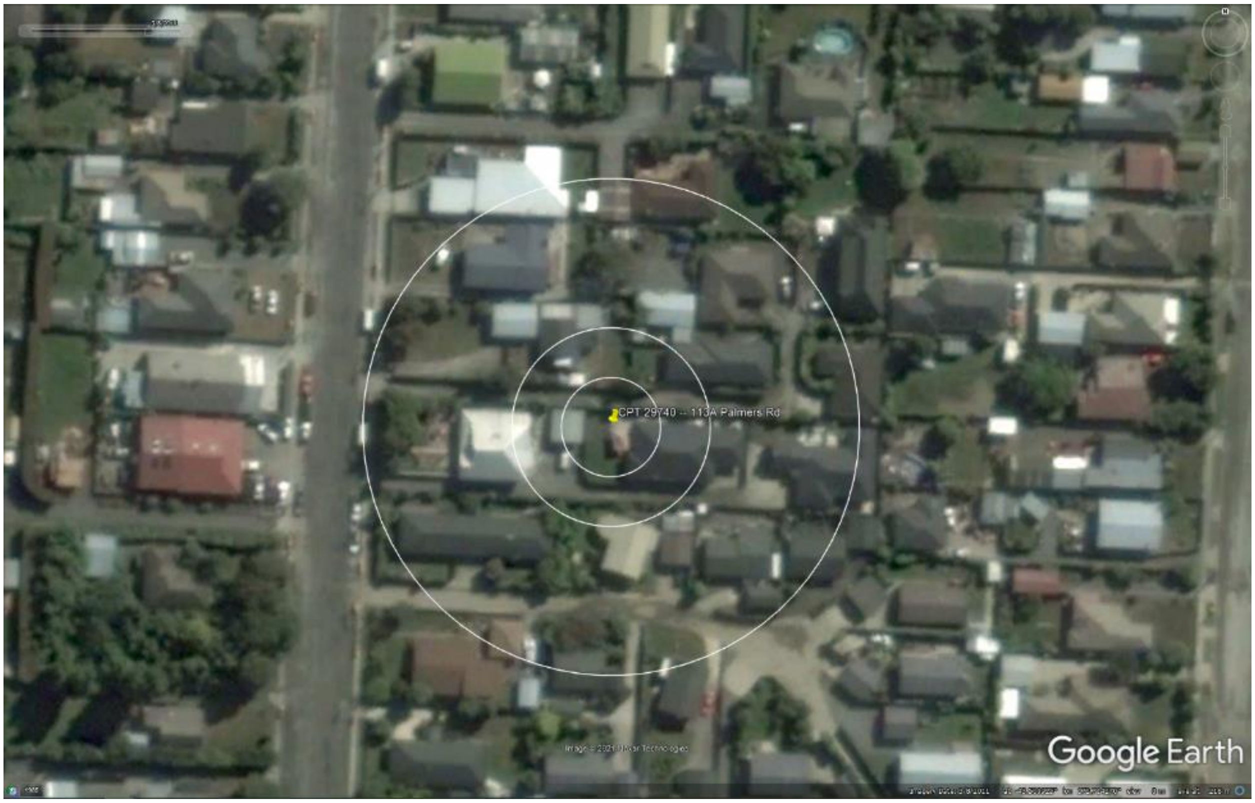

Figure 16: Satellite image of the site taken on Mar 8, 2011.

Figure 17: Satellite image of the site taken in Apr 2012.

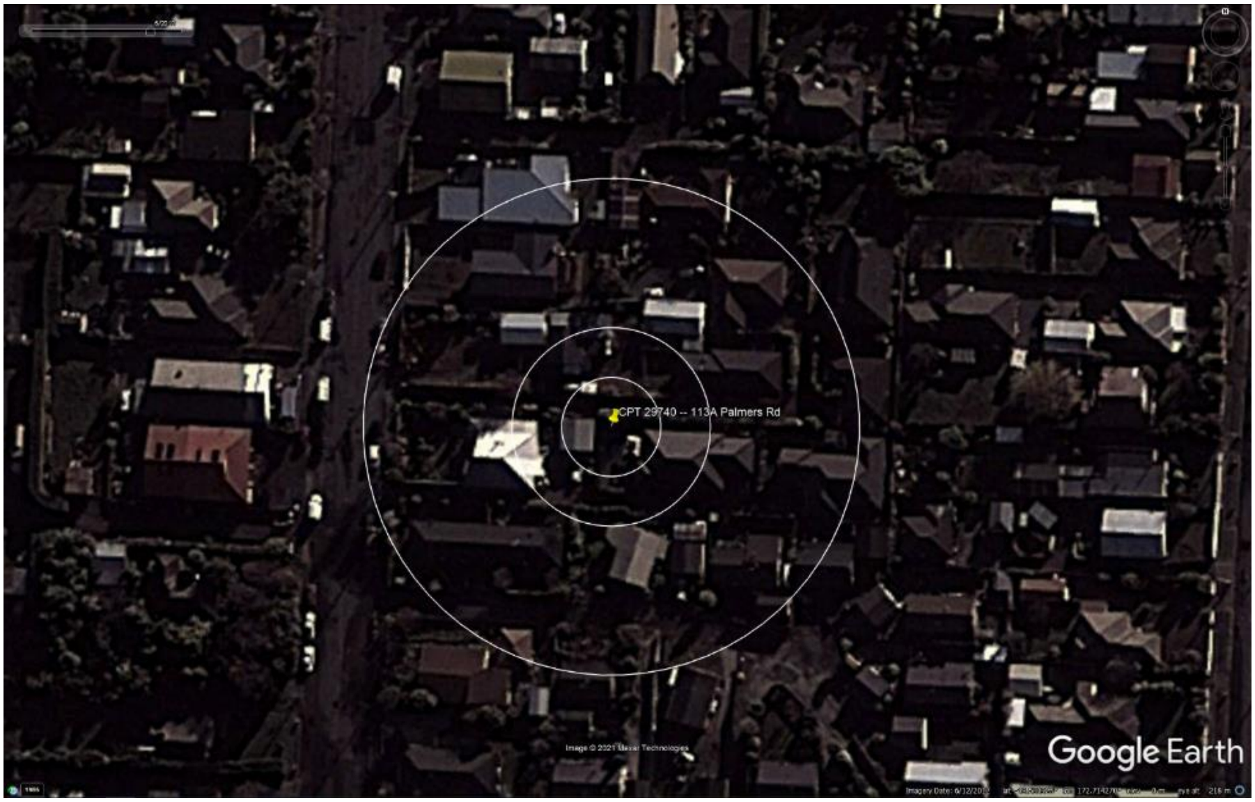

Figure 18: Satellite image of the site taken in Jun 2012.

Figure 19: Satellite image of the site taken in Jan 2013.

Figure 20: Satellite image of the site taken in Mar 2013.

Figure 21: Satellite image of the site taken in Aug 2013.

Figure 22: Satellite image of the site taken in Feb 2014.

Figure 23: Satellite image of the site taken in Sep 2014.

Figure 24: Satellite image of the site taken in Jan 2015.

Figure 25: Satellite image of the site taken in Jun 2015.

Figure 26: Satellite image of the site taken in Nov 2015.

Figure 27: Aerial photograph of the site taken on Sep 4, 2010.

Figure 28: Aerial photograph of the site taken on Feb 24, 2011.

Figure 29: Aerial photograph of the site taken on June 14-15, 2011.

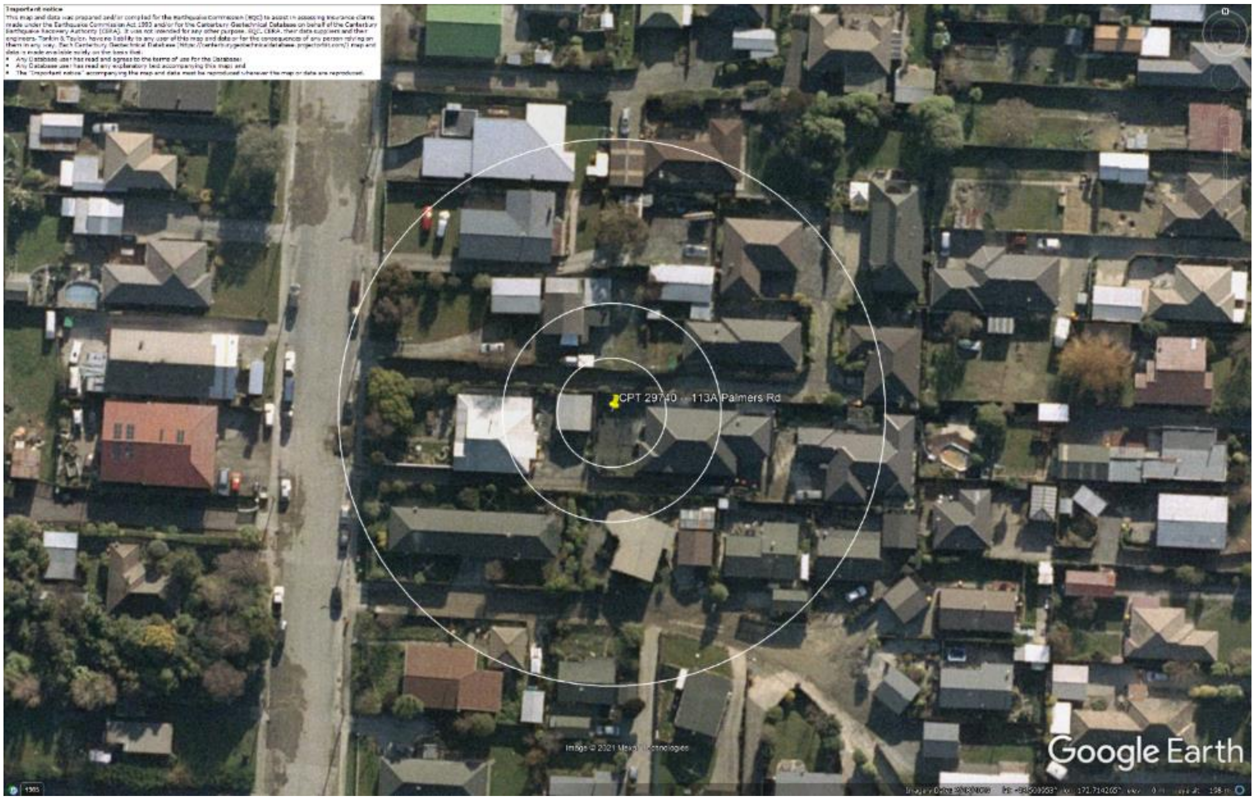

Figure 30: Aerial photograph of the site taken on June 16, 2011.

Figure 31: Aerial photograph of the site taken on Dec 24, 2011.

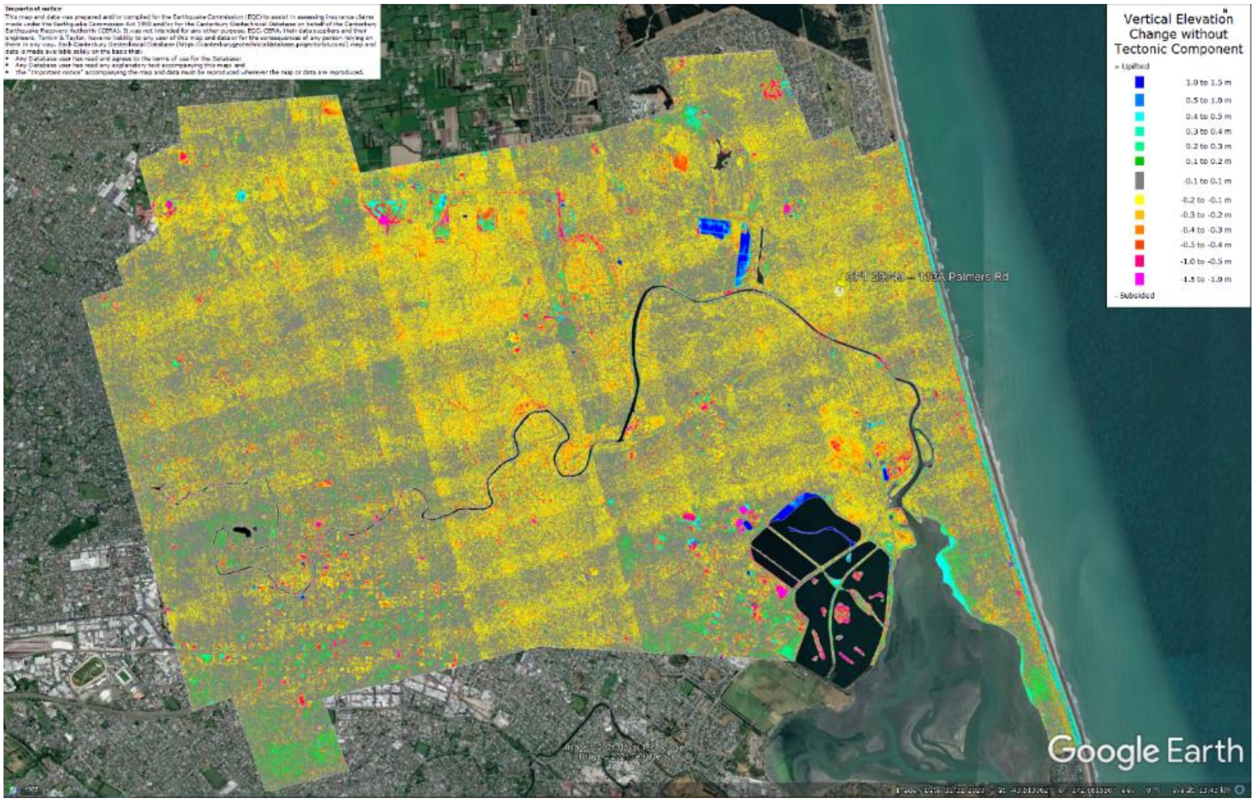

Figure 32: Vertical Ground Movements (Surface – Tectonic) for Sep 2010 Earthquake – the site is not in the apparent zone of overestimated ground surface subsidence.

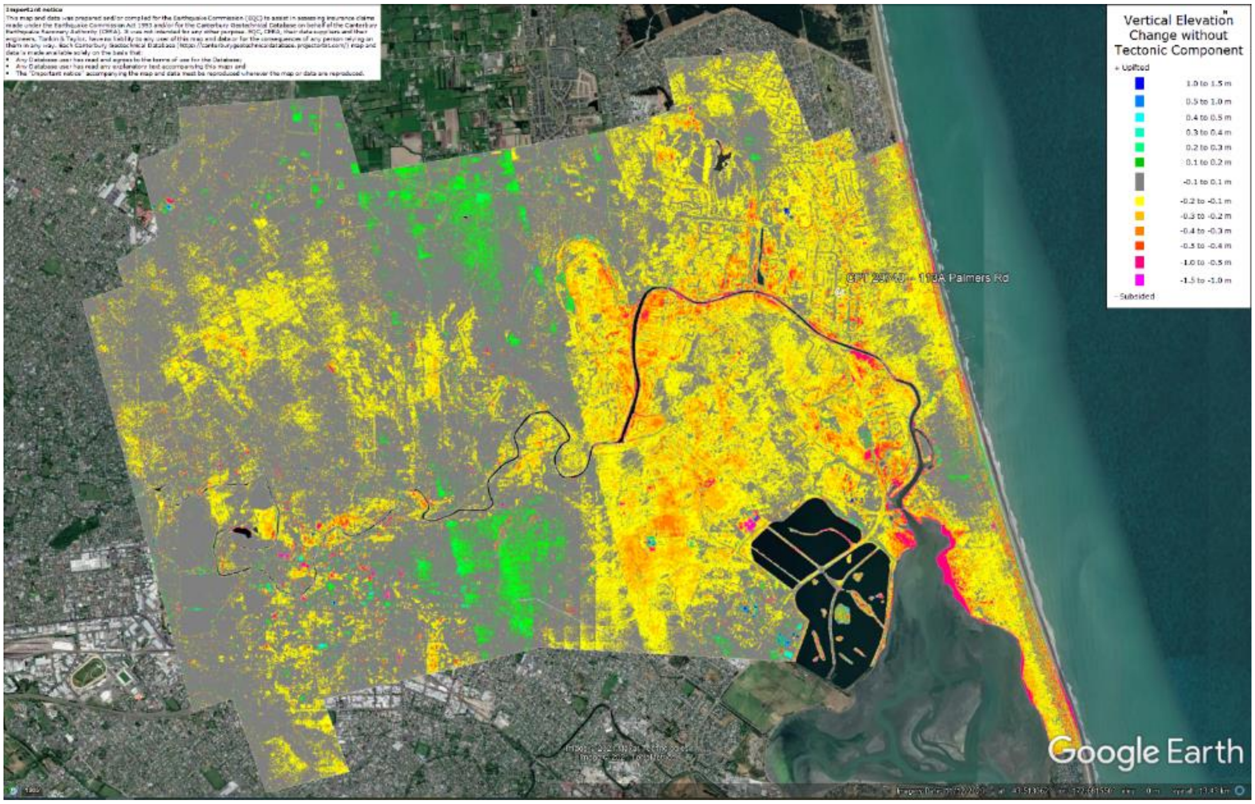

Figure 33: Vertical Ground Movements (Surface – Tectonic) for Feb 2011 Earthquake – the site is not in the apparent zone of underestimated ground surface subsidence.

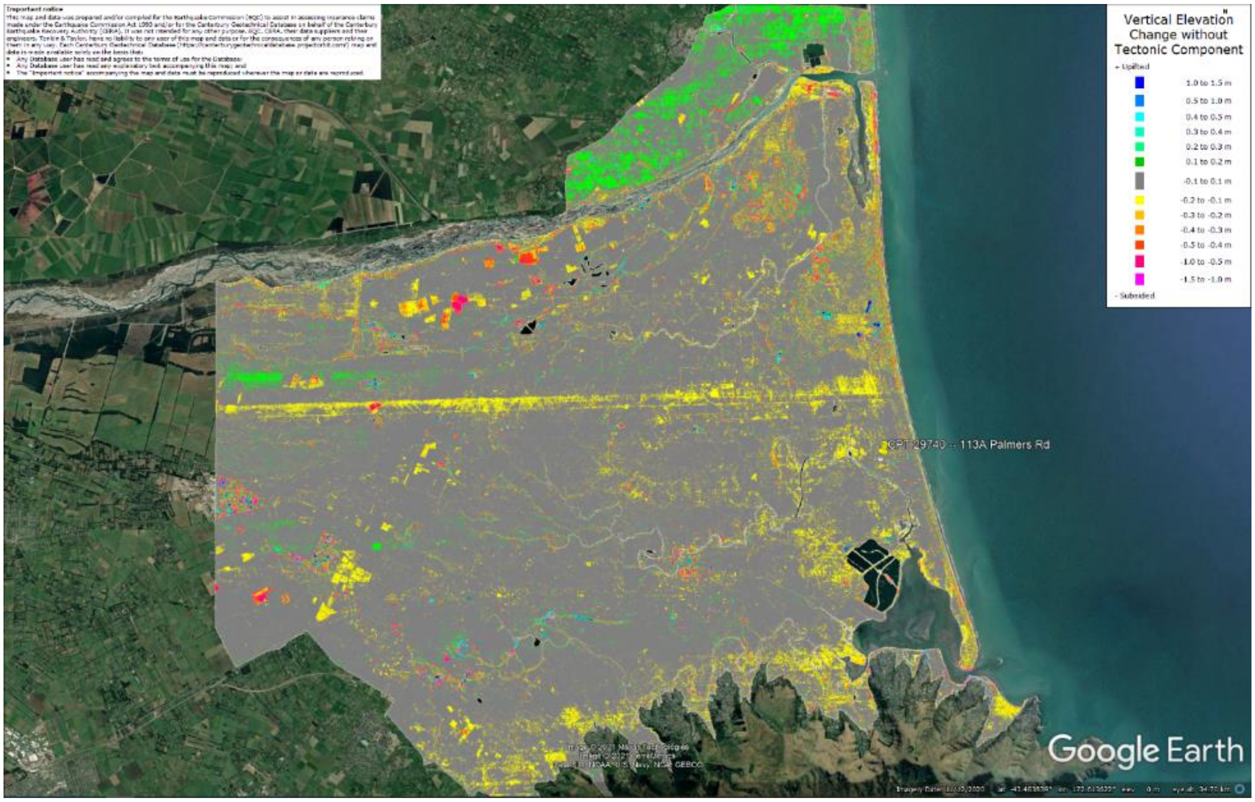

Figure 34: Vertical Ground Movements (Surface – Tectonic) for June 2011 Earthquake – the site is not in the apparent zone of overestimated or underestimated ground surface subsidence.

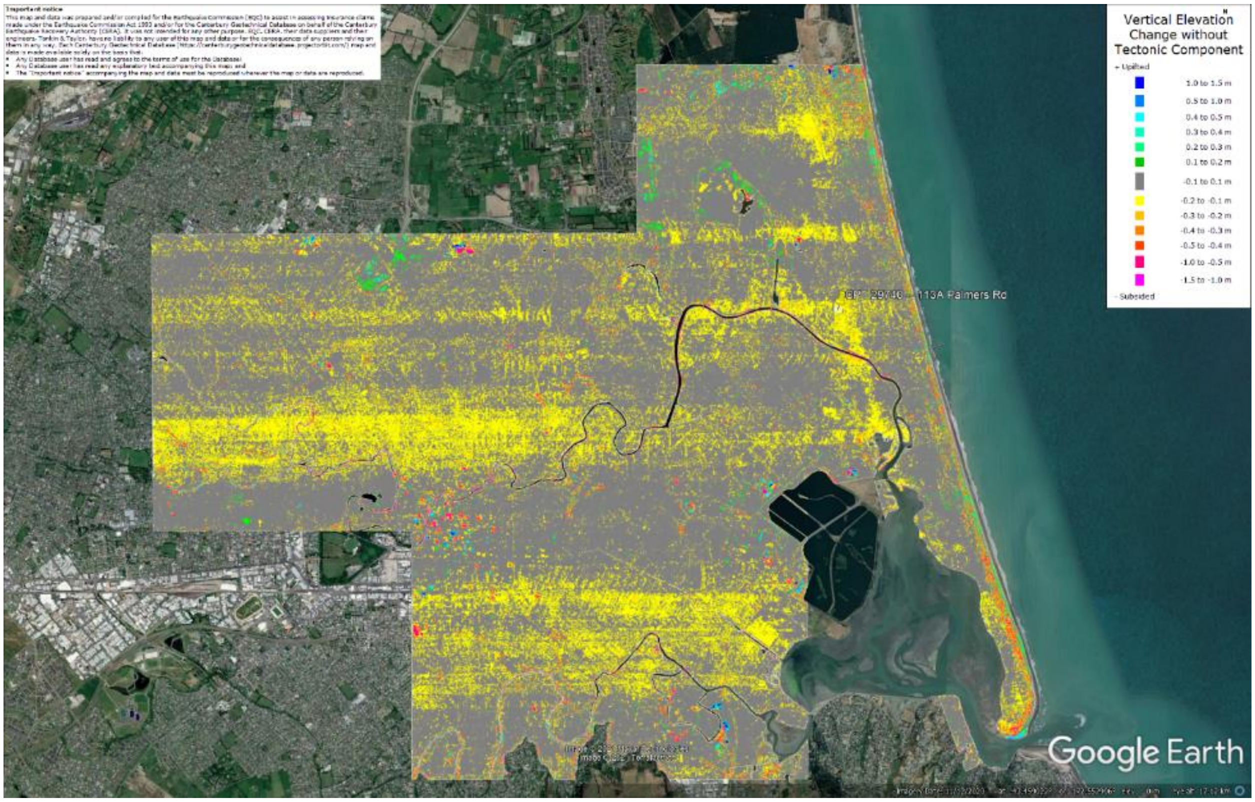

Figure 35: Vertical Ground Movements (Surface – Tectonic) for Dec 2011 Earthquake – the site is in the apparent zone of overestimated ground surface subsidence (i.e., Feb 2012 LiDAR flight band error).

Figure 36: Ground surface subsidence without tectonic component for Sep 2010 Earthquake according to the LiDAR DEM.

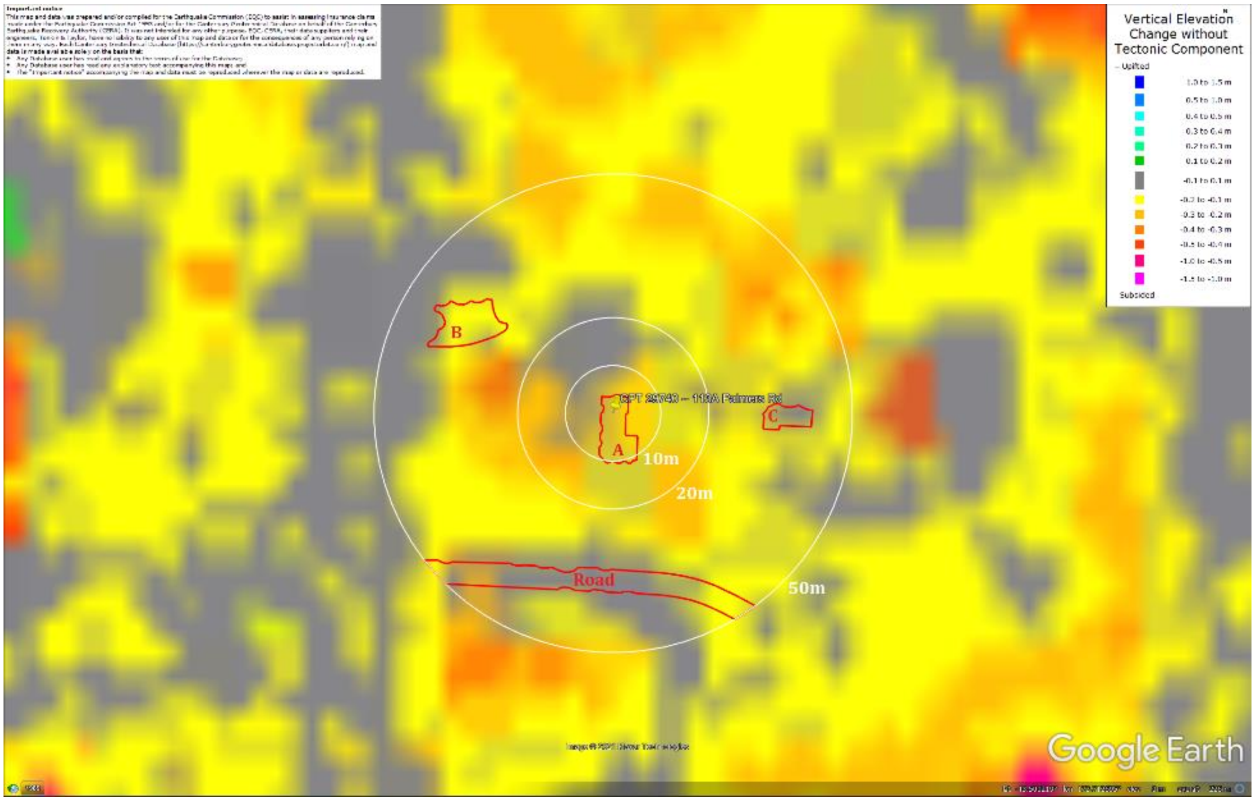

Figure 37: Ground surface subsidence without tectonic component for Feb 2011 Earthquake according to the LiDAR DEM.

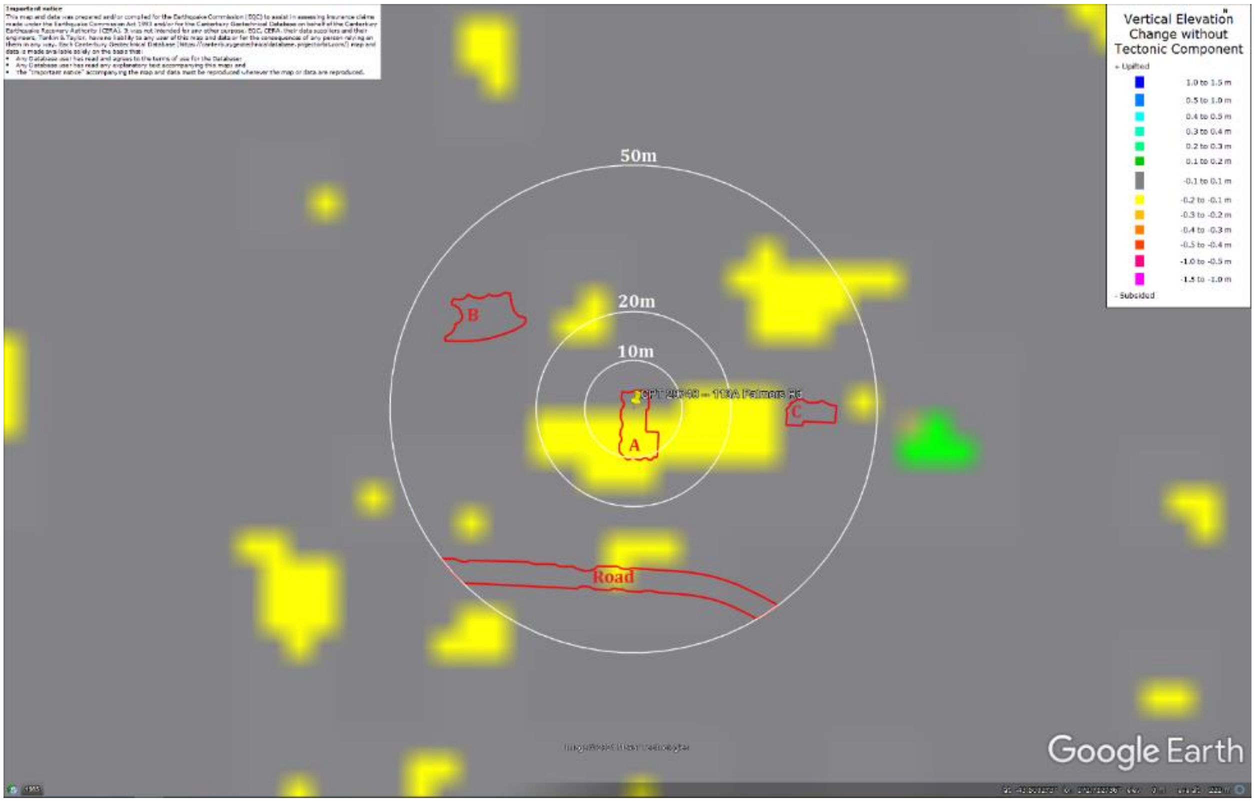

Figure 38: Ground surface subsidence without tectonic component for June 2011 Earthquake according to the LiDAR DEM.

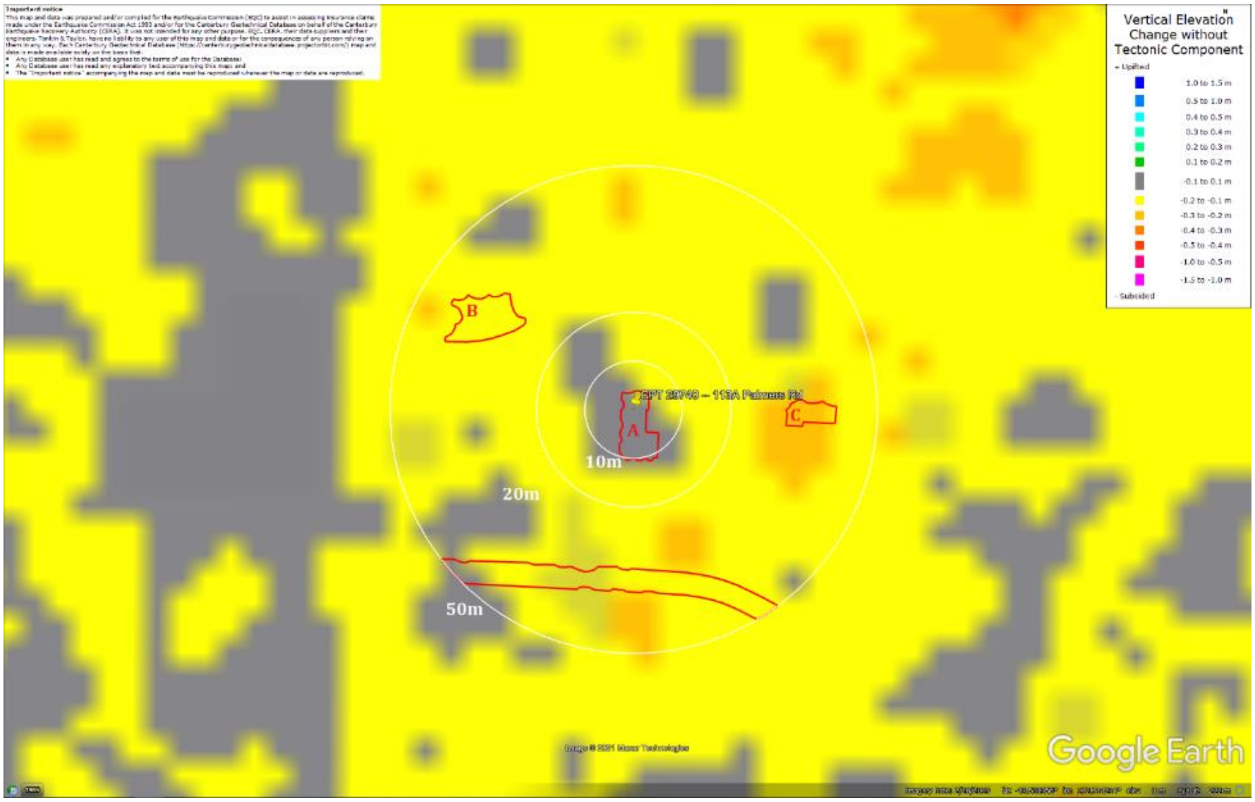

Figure 39: Ground surface subsidence without tectonic component for Dec 2011 Earthquake according to the LiDAR DEM.

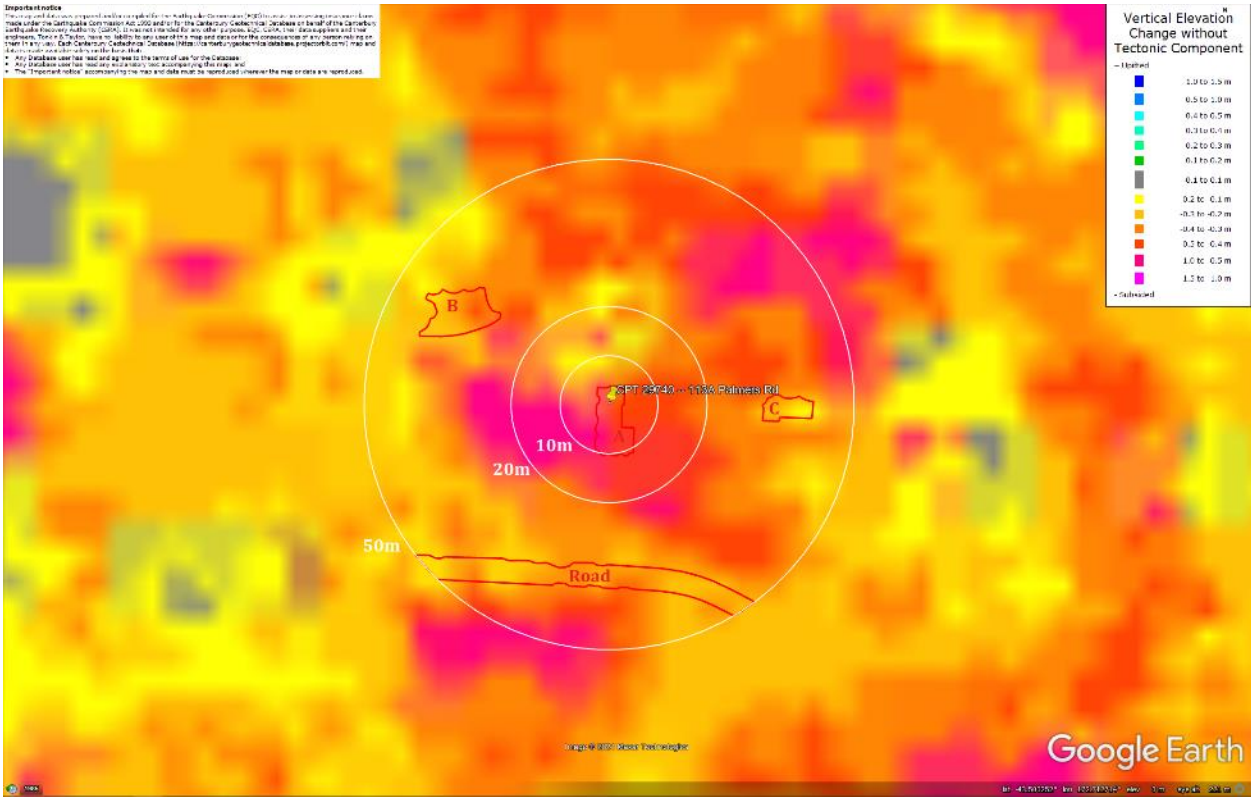

Figure 40: Ground surface subsidence without tectonic component for Feb 2011 + June 2011 + Dec 2011 Earthquakes according to the LiDAR DEM.

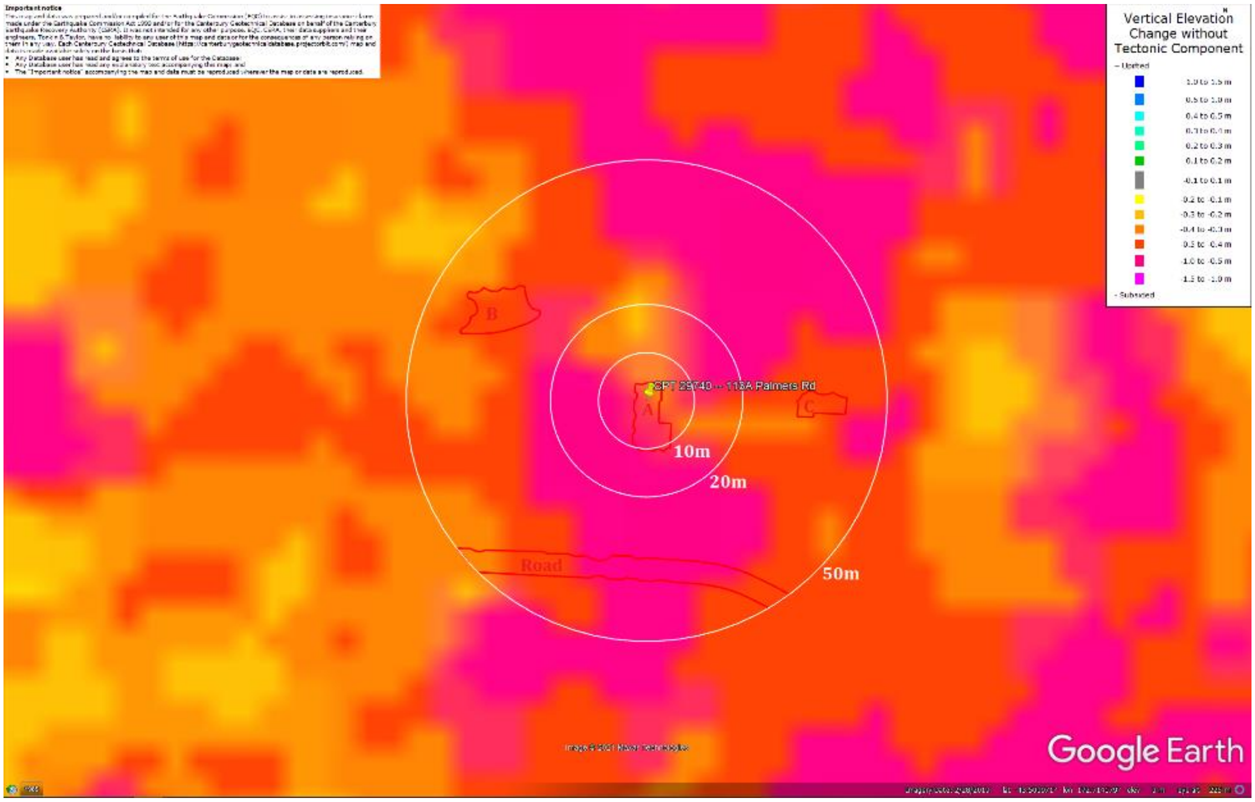

Figure 41: Ground surface subsidence without tectonic component for Canterbury Earthquake Sequence according to the LiDAR DEM.

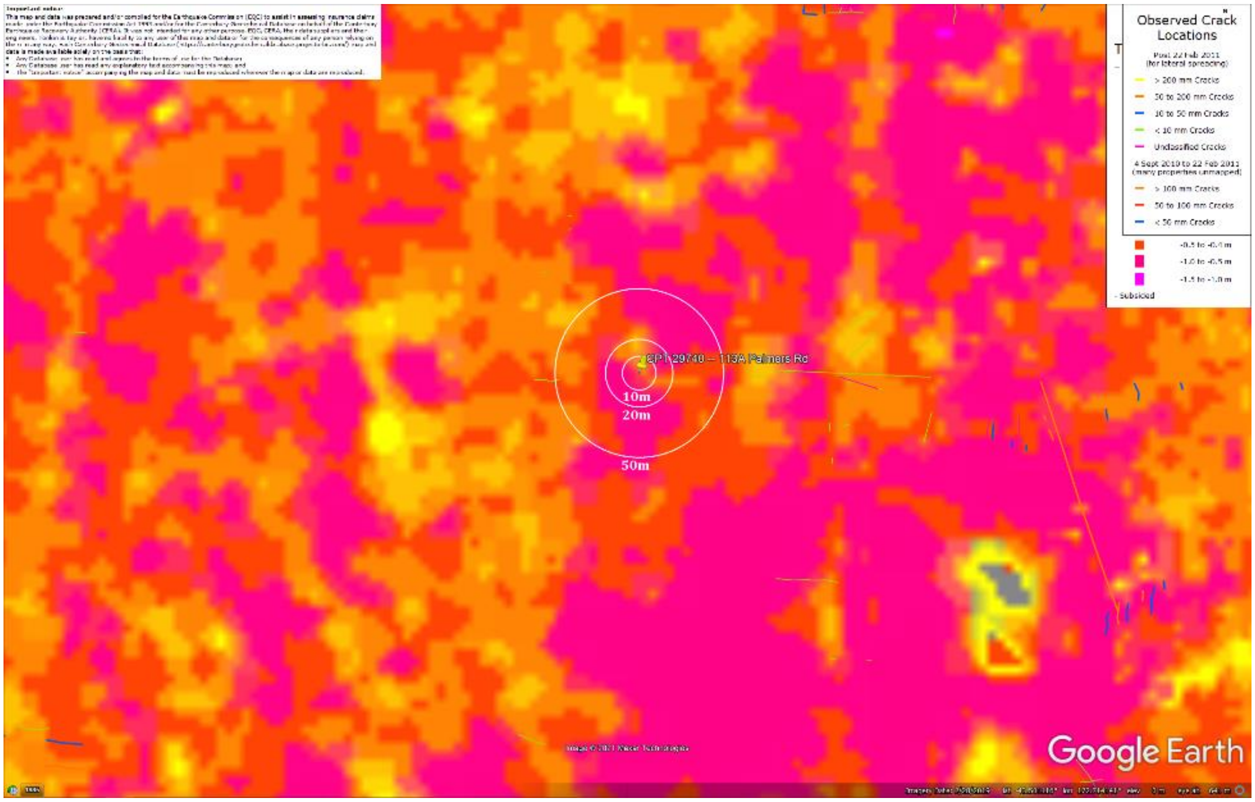

Figure 42: No lateral spreading for Canterbury Earthquake Sequence except local lateral spreading in the E portion of the 50-m buffer.

Figure 43: Vertical tectonic movements for Sep 2010 Earthquake.

Figure 44: Vertical tectonic movements for Feb 2011 Earthquake.

Figure 45: Vertical tectonic movements for June 2011 Earthquake.

Figure 46: Vertical tectonic movements for Dec 2011 Earthquake.

Figure 47: Vertical tectonic movements for Canterbury Earthquake Sequence.

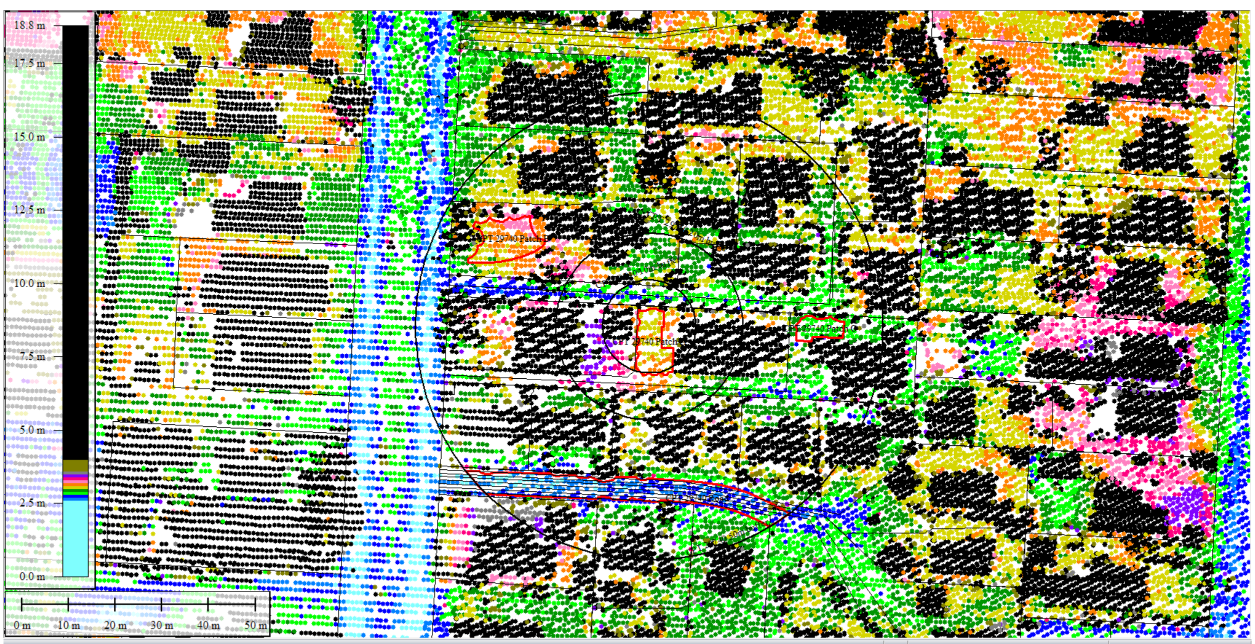

Figure 48: Sep 5, 2010 LiDAR survey.

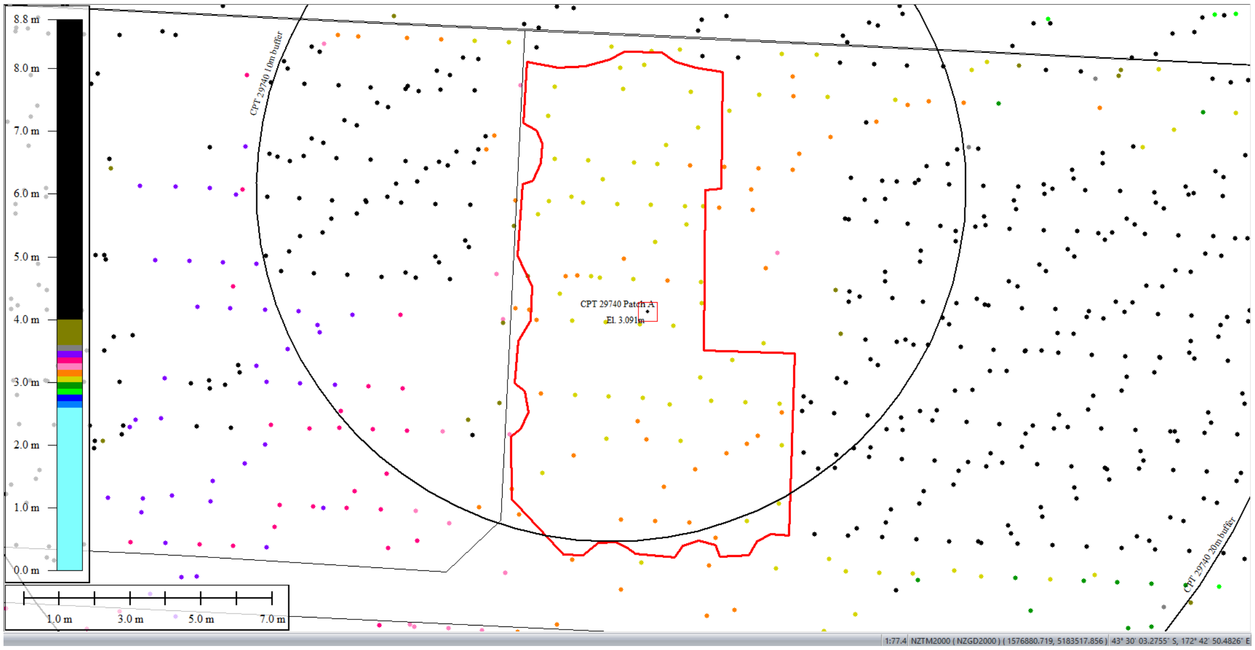

Figure 49: Ground surface elevation averaged over 10-m, 20-m, and 50-m buffers for Patch A for Sep 5, 2010 LiDAR survey.

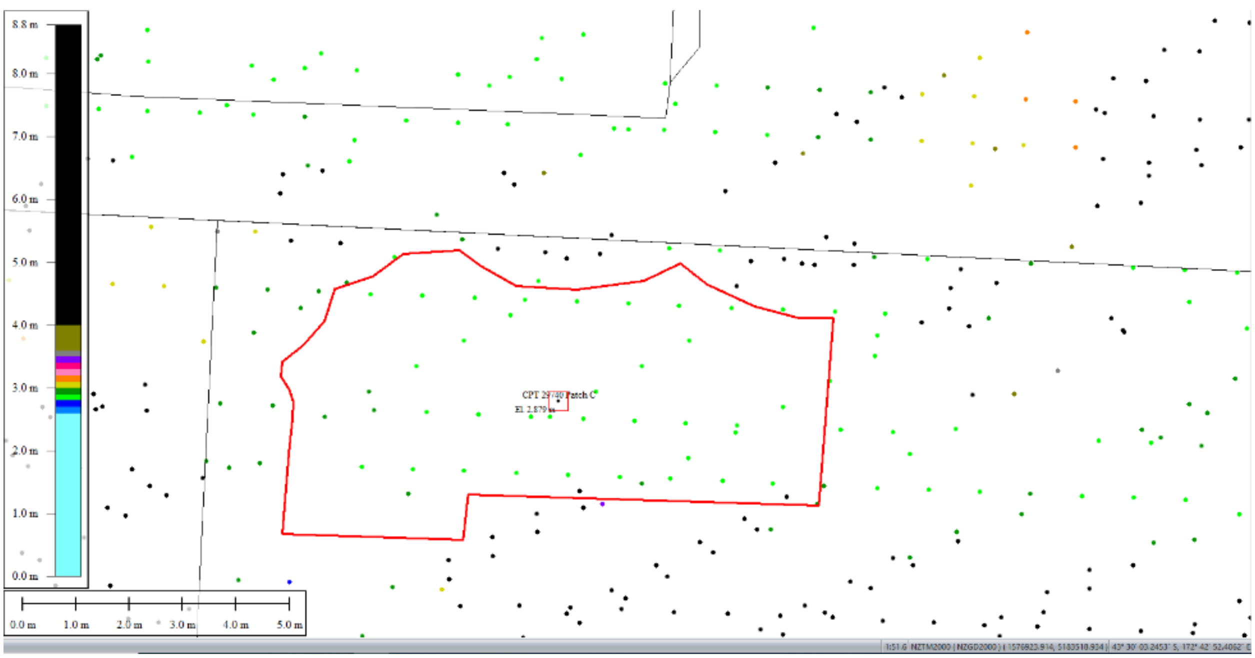

Figure 50: Ground surface elevation averaged over 50-m buffer for Patch C for Sep 5, 2010 LiDAR survey.

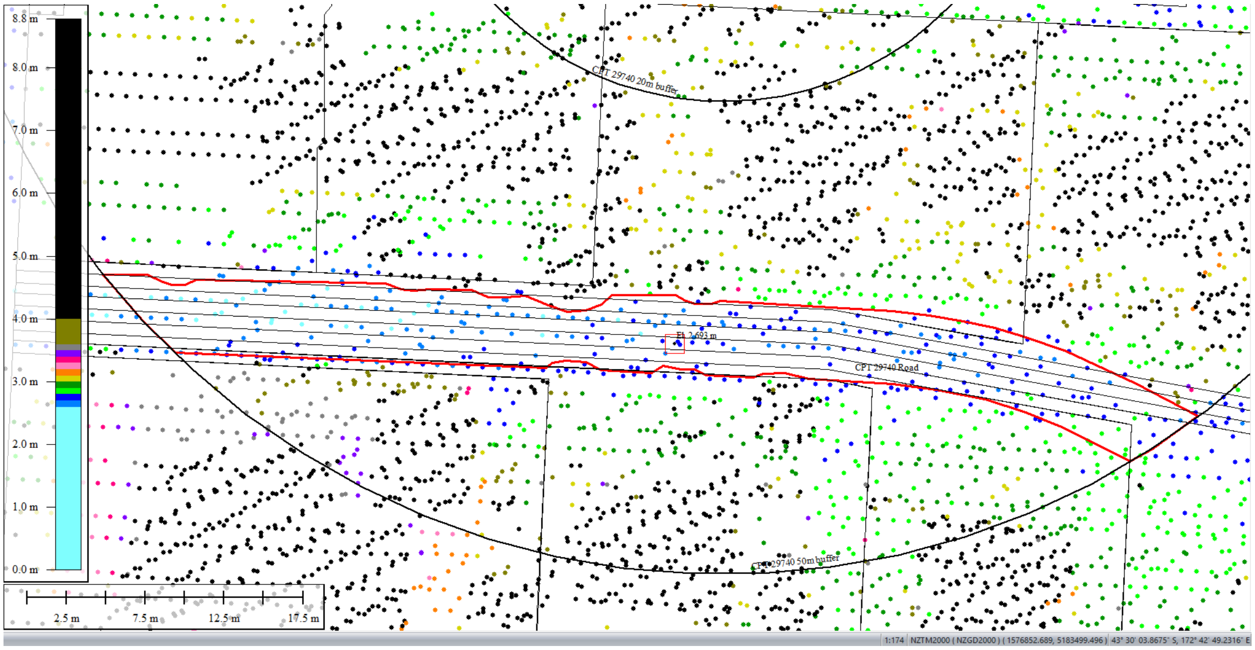

Figure 51: Ground surface elevation averaged over 50-m buffer for Road for Sep 5, 2010 LiDAR survey.

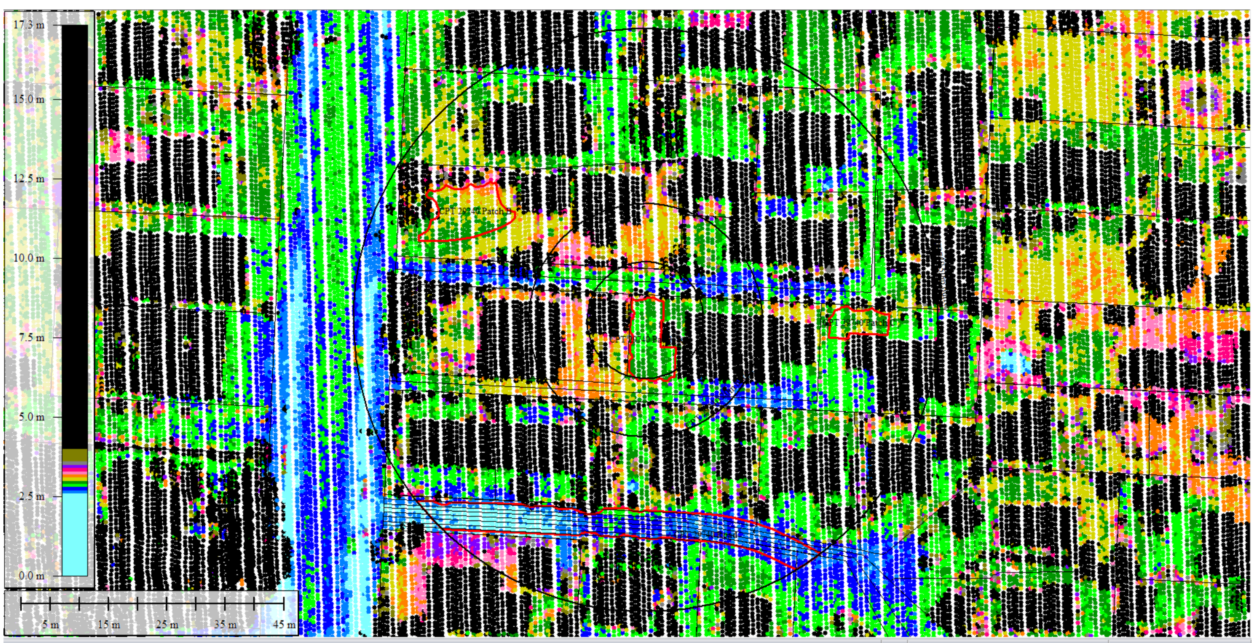

Figure 52: Mar 2011 LiDAR survey.

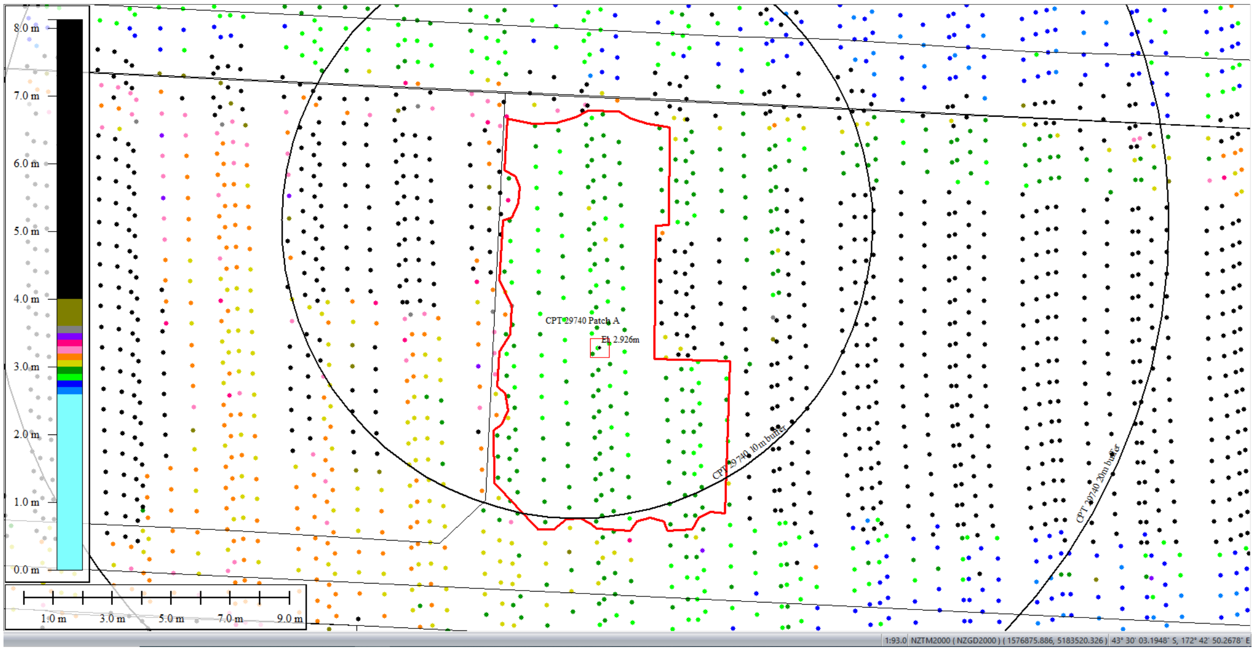

Figure 53: Ground surface elevation averaged over 10-m, 20-m, and 50-m buffers for Patch A for Mar 2011 LiDAR survey.

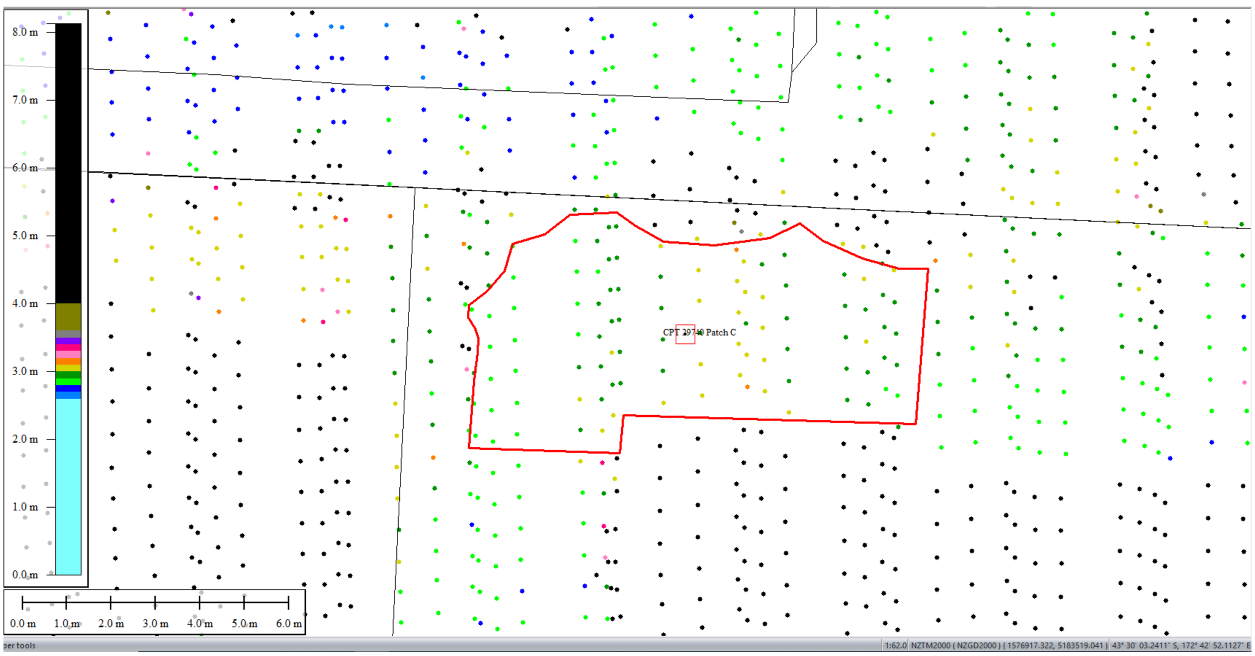

Figure 54: Ground surface elevation averaged over 50-m buffer for Patch C for Mar 2011 LiDAR survey (el. 2.963m).

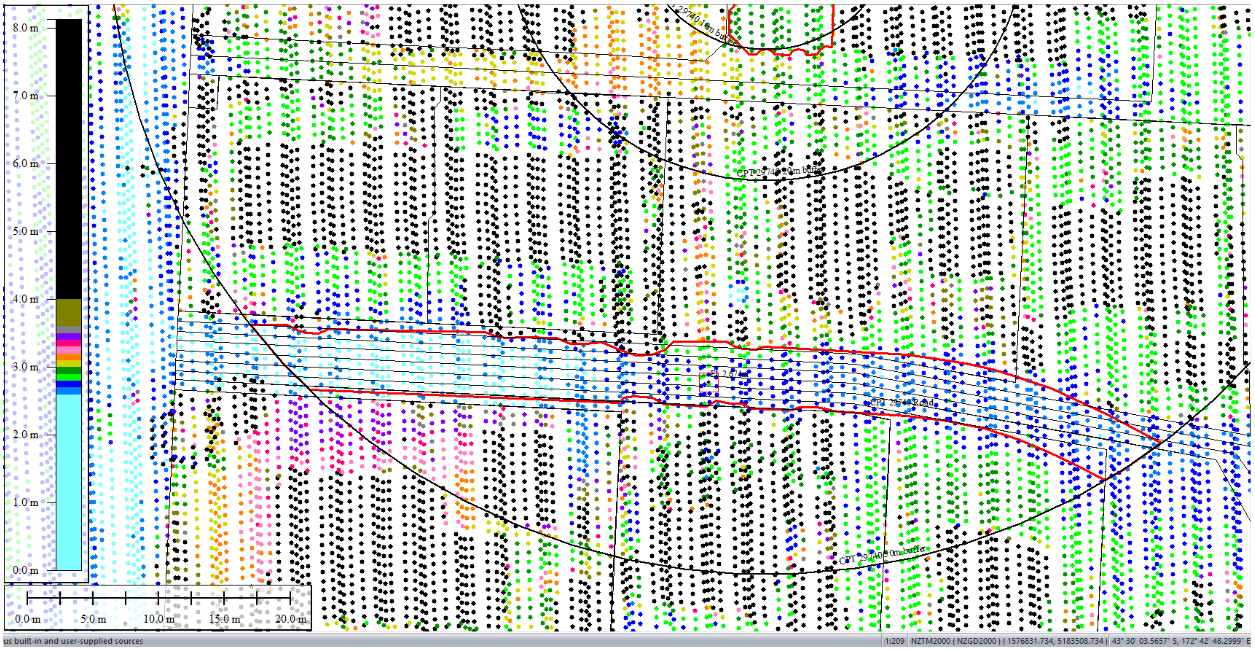

Figure 55: Ground surface elevation averaged over 50-m buffer for Road for Mar 2011 LiDAR survey.

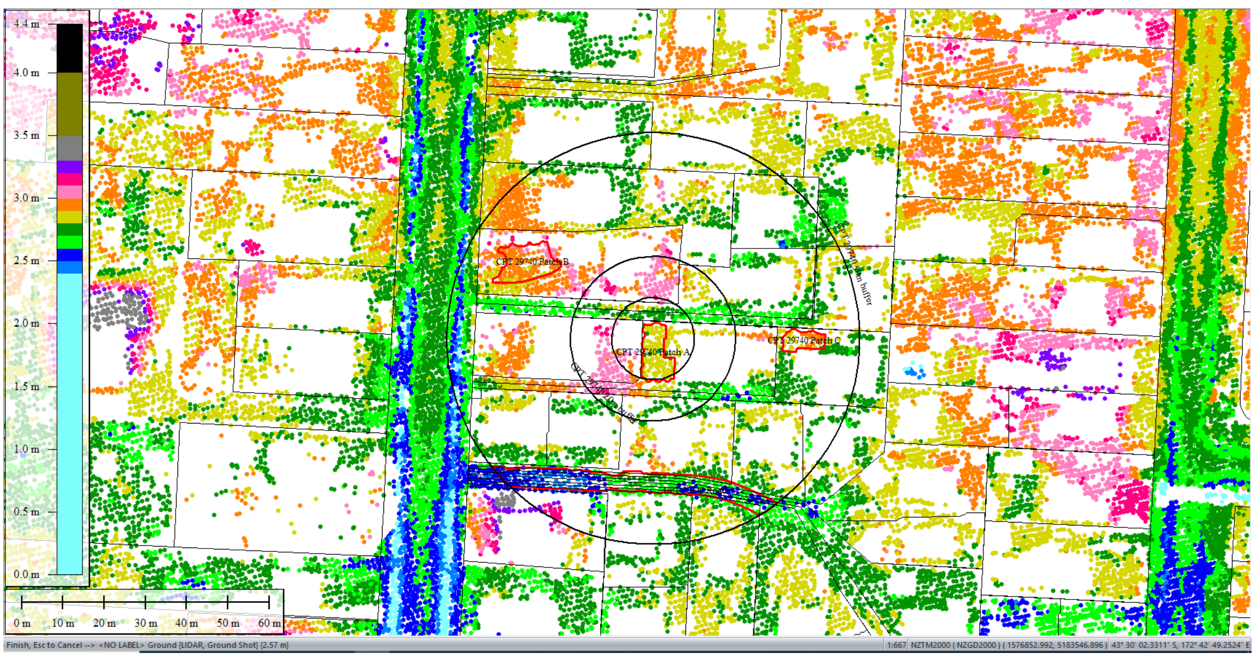

Figure 56: May 2011 LiDAR survey.

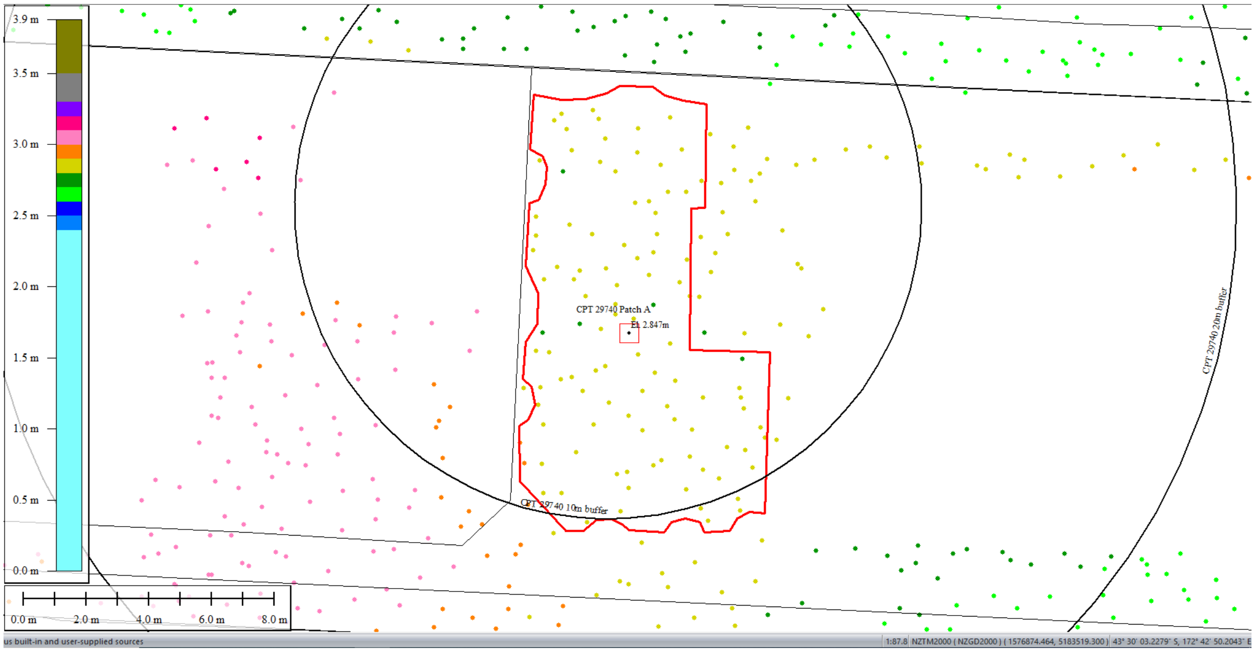

Figure 57: Ground surface elevation averaged over 10-m, 20-m, and 50-m buffers for Patch A for May 2011 LiDAR survey.

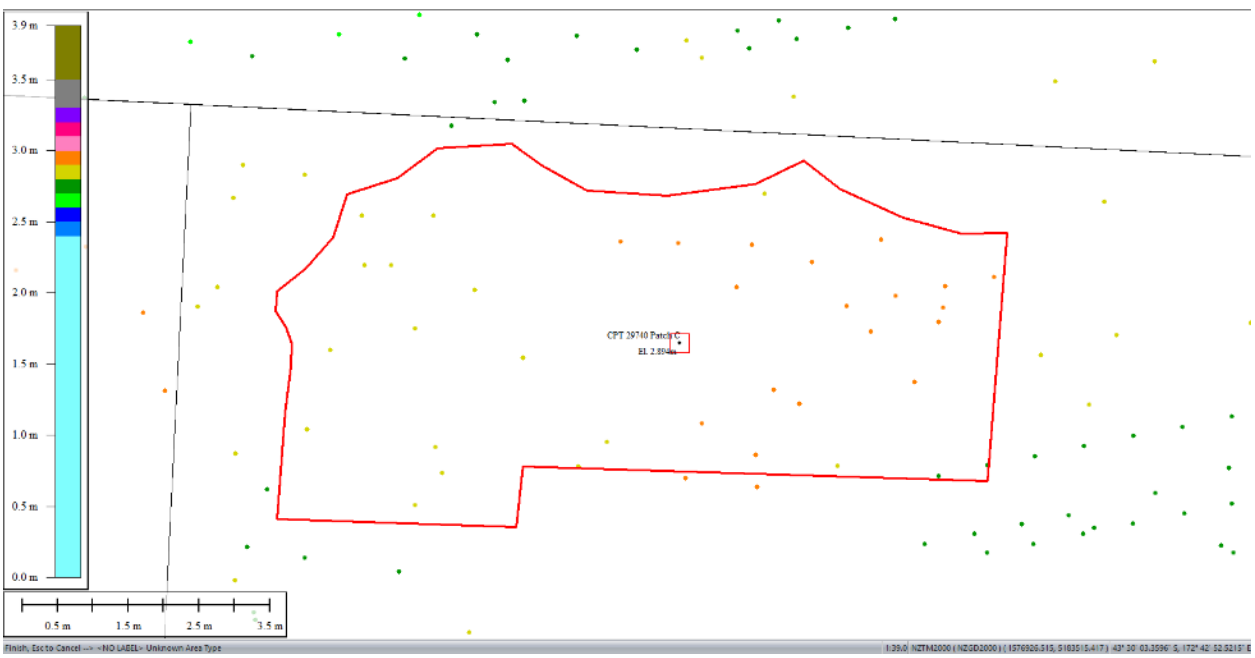

Figure 58: Ground surface elevation averaged over 50-m buffer for Patch C for May 2011 LiDAR survey.

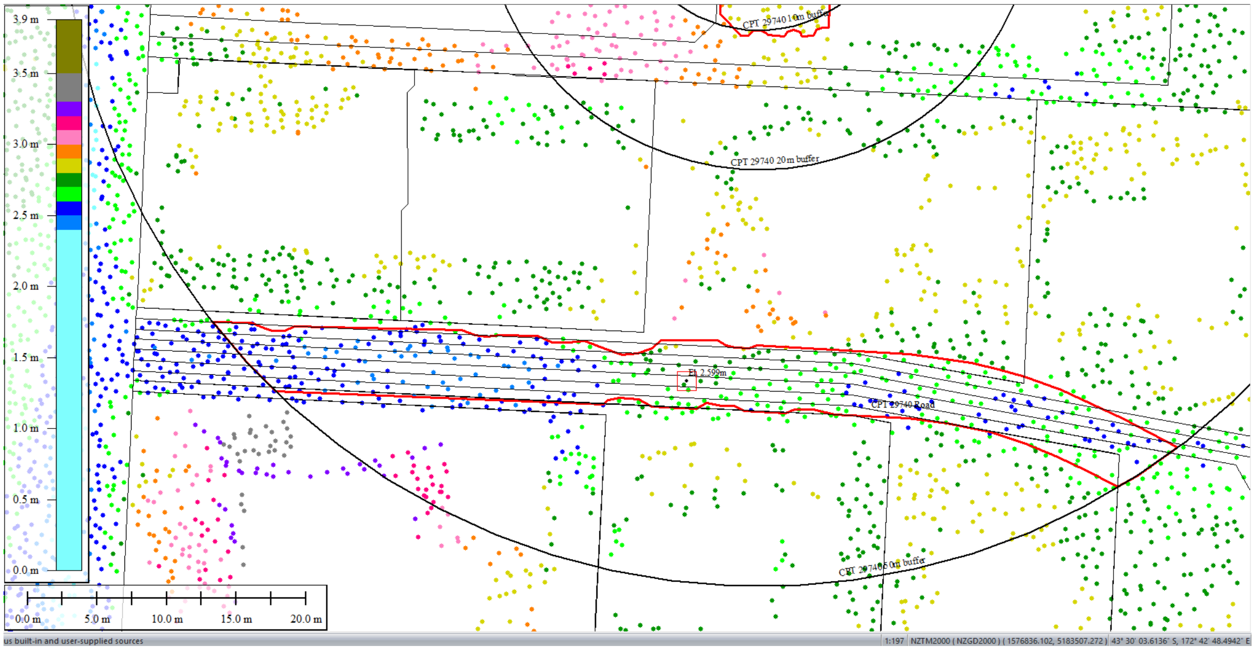

Figure 59: Ground surface elevation averaged over 50-m buffer for Road for May 2011 LiDAR survey.

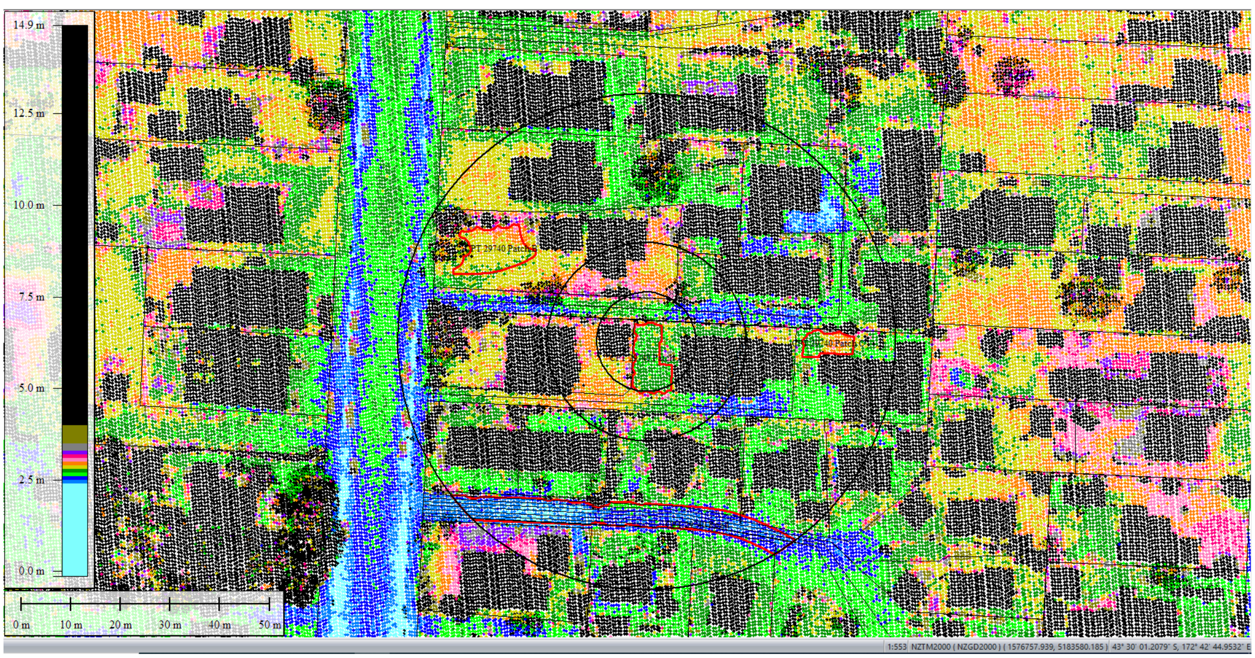

Figure 60: Sep 2011 LiDAR survey.

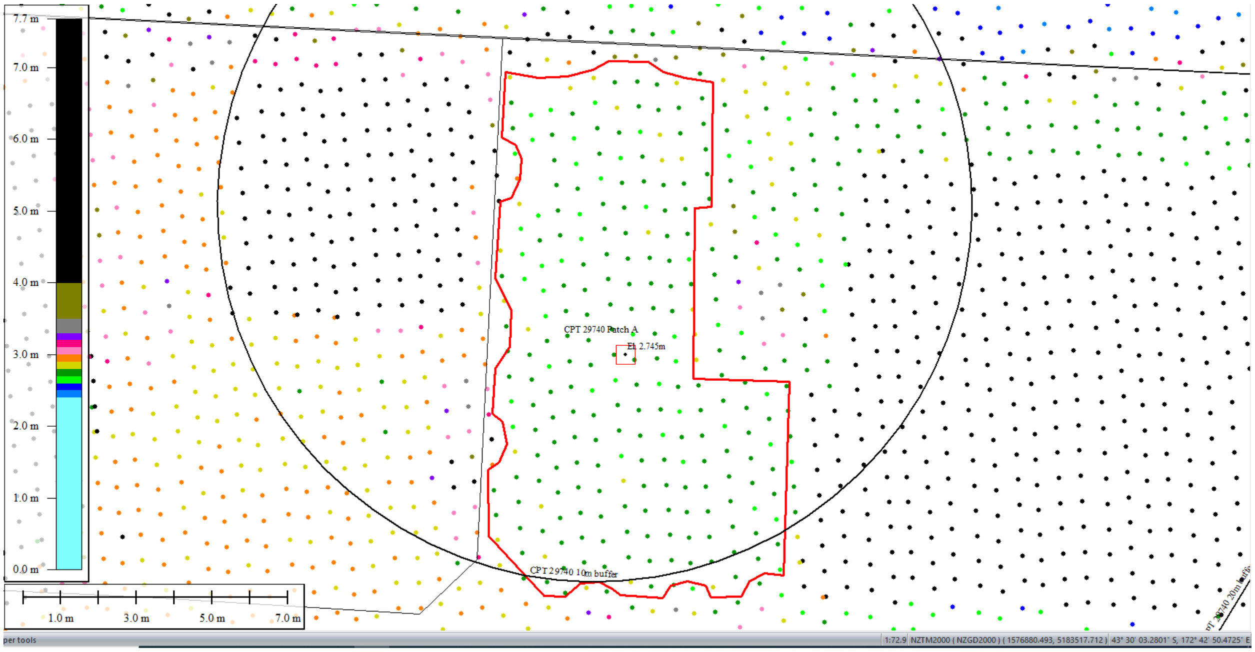

Figure 61: Ground surface elevation averaged over 10-m, 20-m, and 50-m buffers for Patch A for Sep 2011 LiDAR survey.

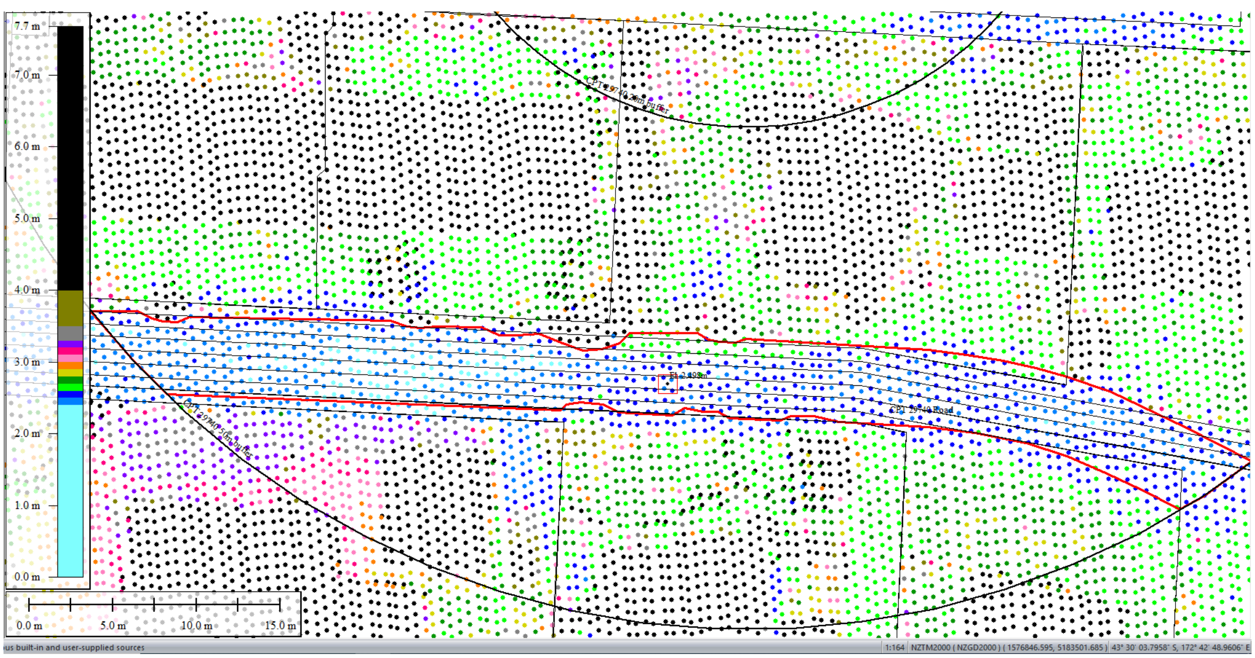

Figure 62: Ground surface elevation averaged over 50-m buffer for Road for Sep 2011 LiDAR survey.

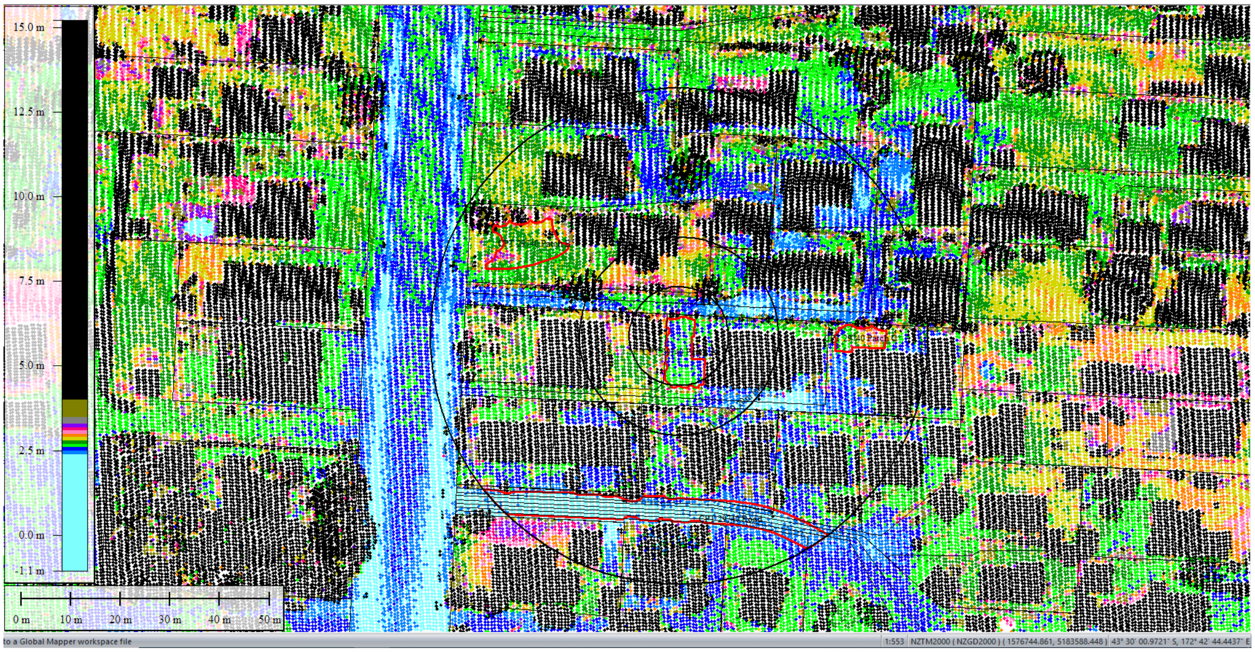

Figure 63: Feb 2012 LiDAR survey.

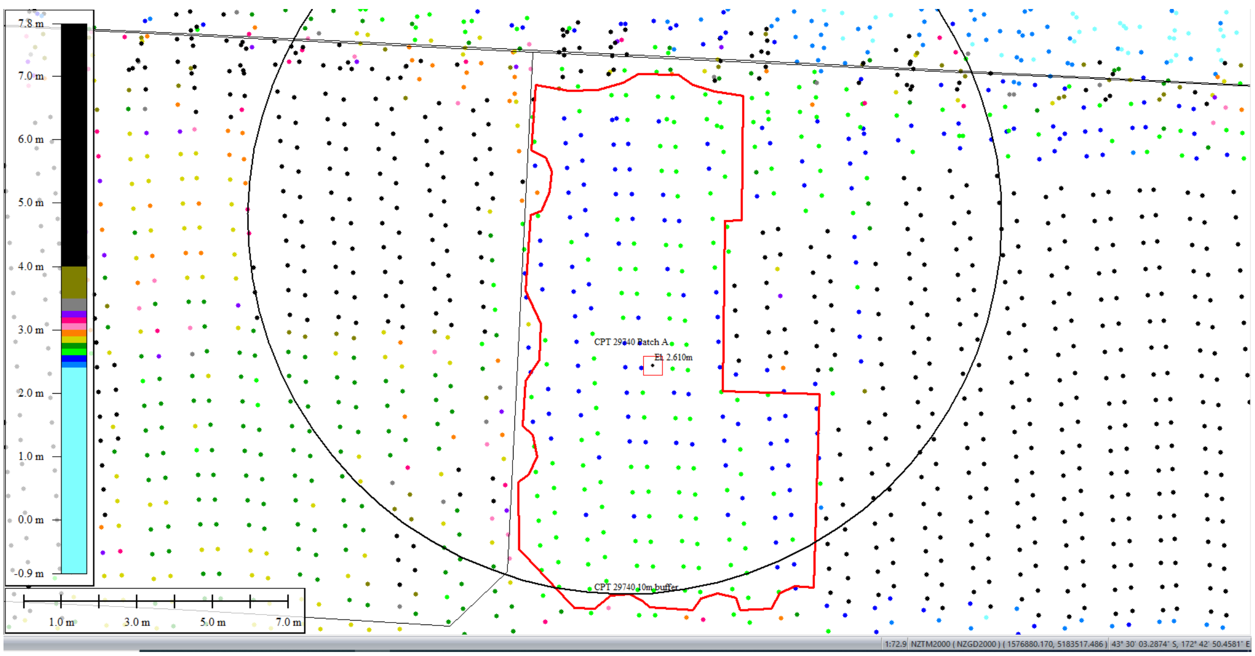

Figure 64: Ground surface elevation averaged over 10-m, 20-m, and 50-m buffers for Patch A for Feb 2012 LiDAR survey.

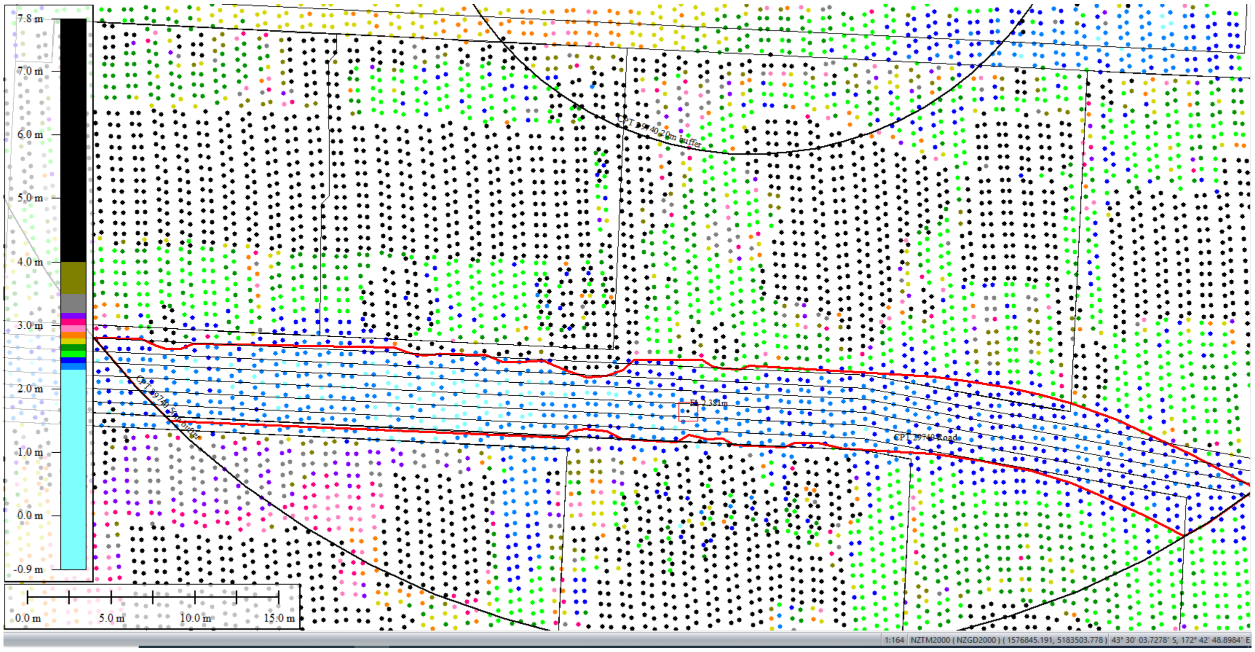

Figure 65: Ground surface elevation averaged over 50-m buffer for Road for Feb 2012 LiDAR survey.

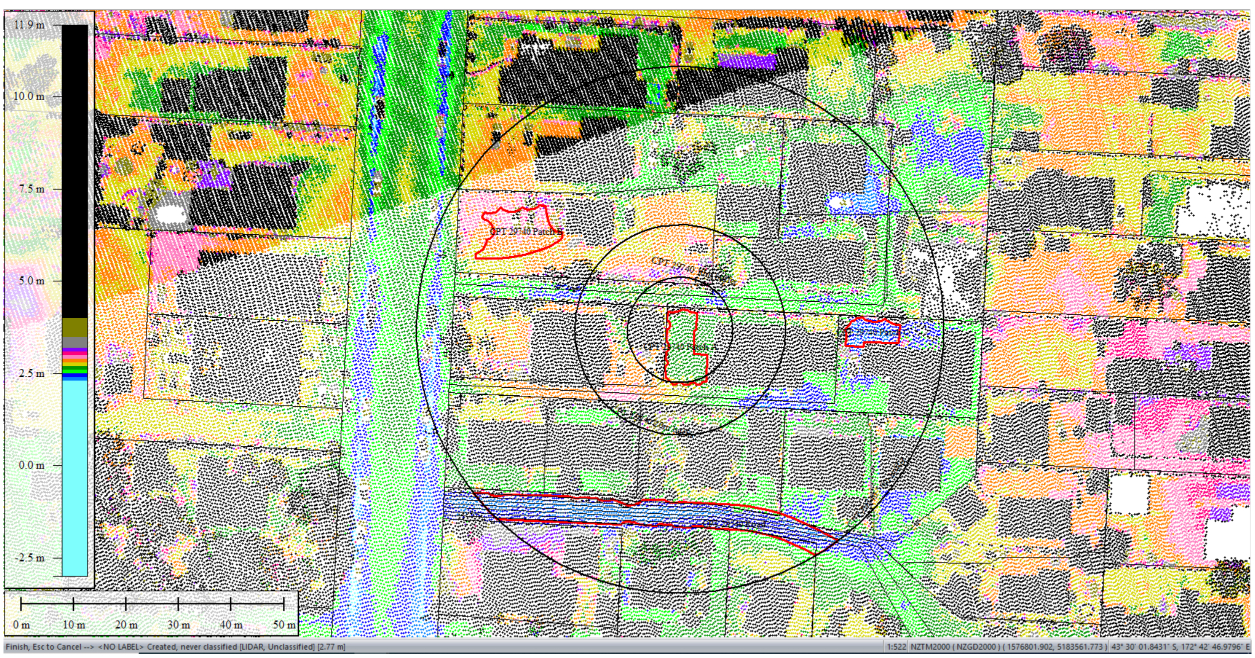

Figure 66: Oct 2015 LiDAR survey.

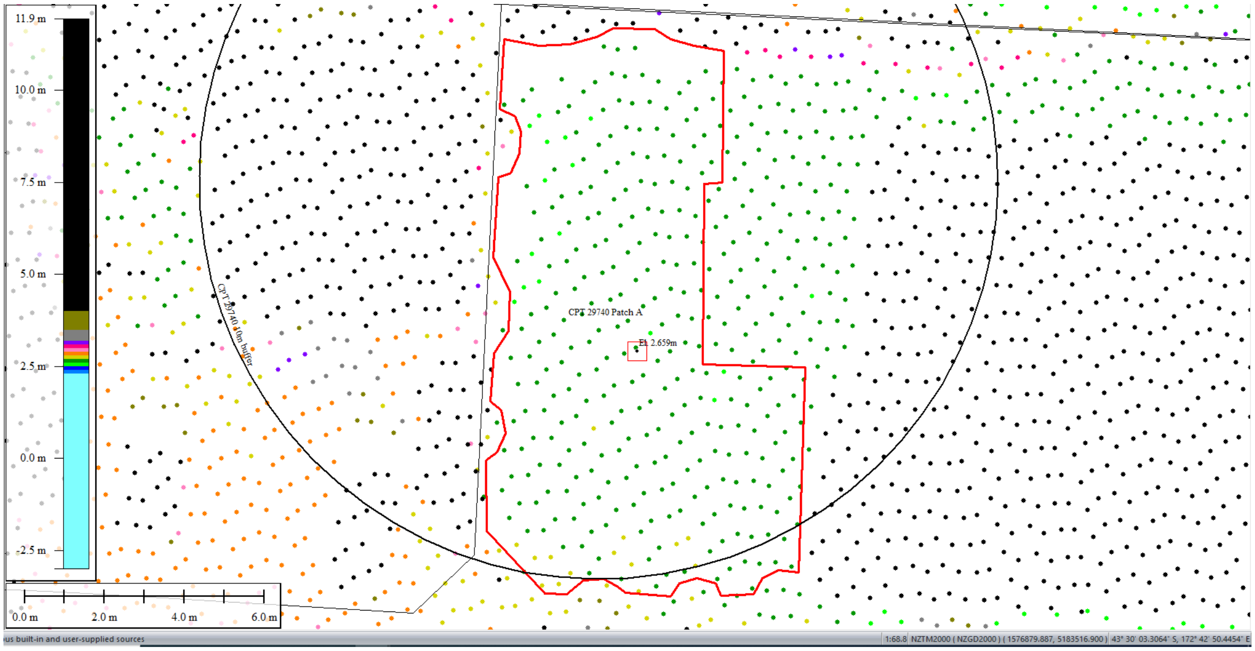

Figure 67: Ground surface elevation averaged over 10-m, 20-m, and 50-m buffers for Patch A for Oct 2015 LiDAR survey.

Figure 68: Aerial photograph showing the ejecta outline at the site for Feb-11 EQ.

Figure 69: Aerial photograph acquired on 16 Jun 2011 showing the ejecta outline at the site for Jun-11 EQ.

Figure 70: Aerial photograph showing the ejecta outline at the site for Dec-11 EQ.

Contents of this figure cannot be shared as doing so is restricted by a Non-Disclosure Agreement.

Figure 71: LDAT inspection notes for the property with Patch A (inspection date: 31 May 2011).

Figure 72: Ground photographs showing the property with Patch A and ejecta remnants within Patch A (photograph date: Nov 2011).

Contents of this figure cannot be shared as doing so is restricted by a Non-Disclosure Agreement.

Figure 73: LDAT inspection notes for the property with Patch B (inspection date: 9 June 2011). Ejecta were not observed within Patch B.

Figure 74: Ground photographs showing the property with Patch B and no ejecta within Patch B (photograph date: Nov 2011).

Contents of this figure cannot be shared as doing so is restricted by a Non-Disclosure Agreement.

Figure 75: LDAT inspection notes for the property with Patch C (inspection date: 31 May 2011).

Figure 76: Ground photographs showing the property with Patch C and ejecta remnants within Patch C (photograph date: 31 May 2011).

Contents of this figure cannot be shared as doing so is restricted by a Non-Disclosure Agreement.

Figure 77: LDAT inspection notes for the property with Patch C (inspection date: July 2011). The Jun-11 EQ caused lateral spreading at the property. The width of the ground cracks exceeded 100 mm.

Figure 78: Ground photographs showing the property with Patch C and ejecta remnants within Patch C (photograph date: July 2011). The ground underwent lateral spreading.

Figure 79: Ground photographs showing ejecta remnants at the properties within the 50-m buffer (photograph date: 9 June 2011).

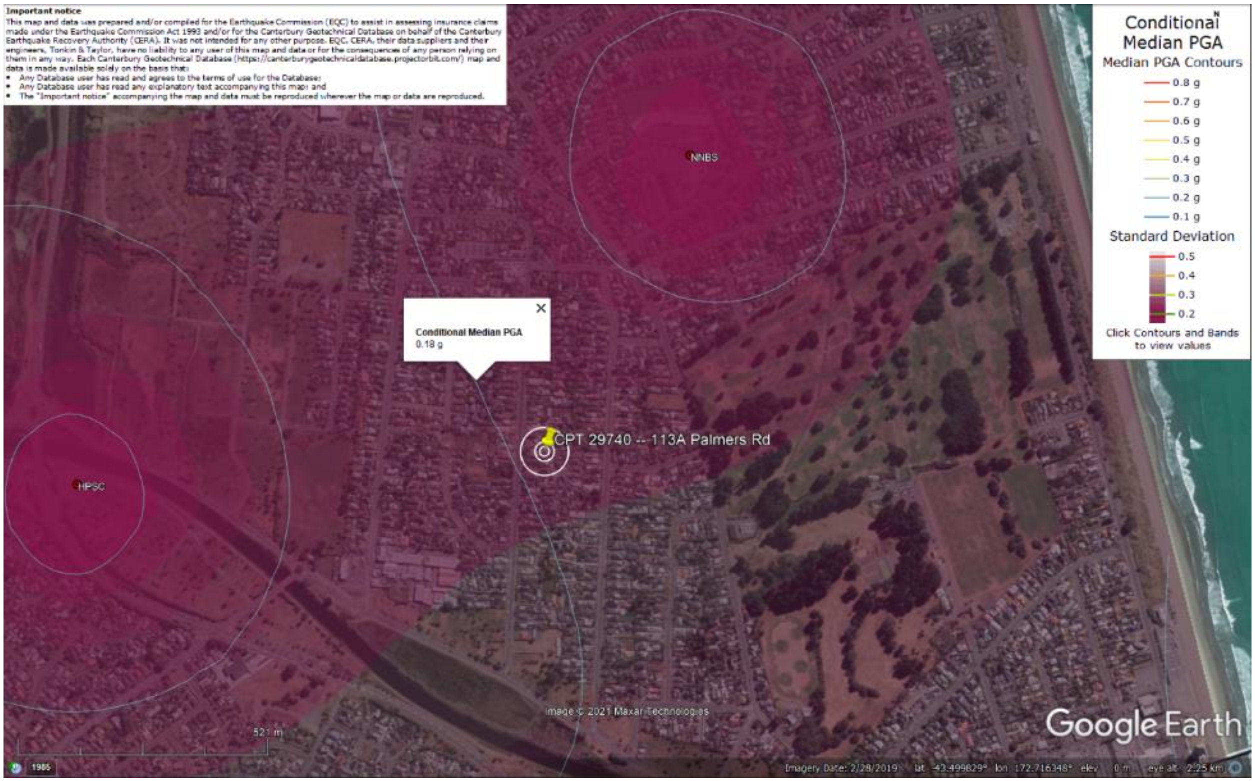

Figure 80: PGA for Sep-10 EQ (st. dev. = 0.250-0.275 ln units).

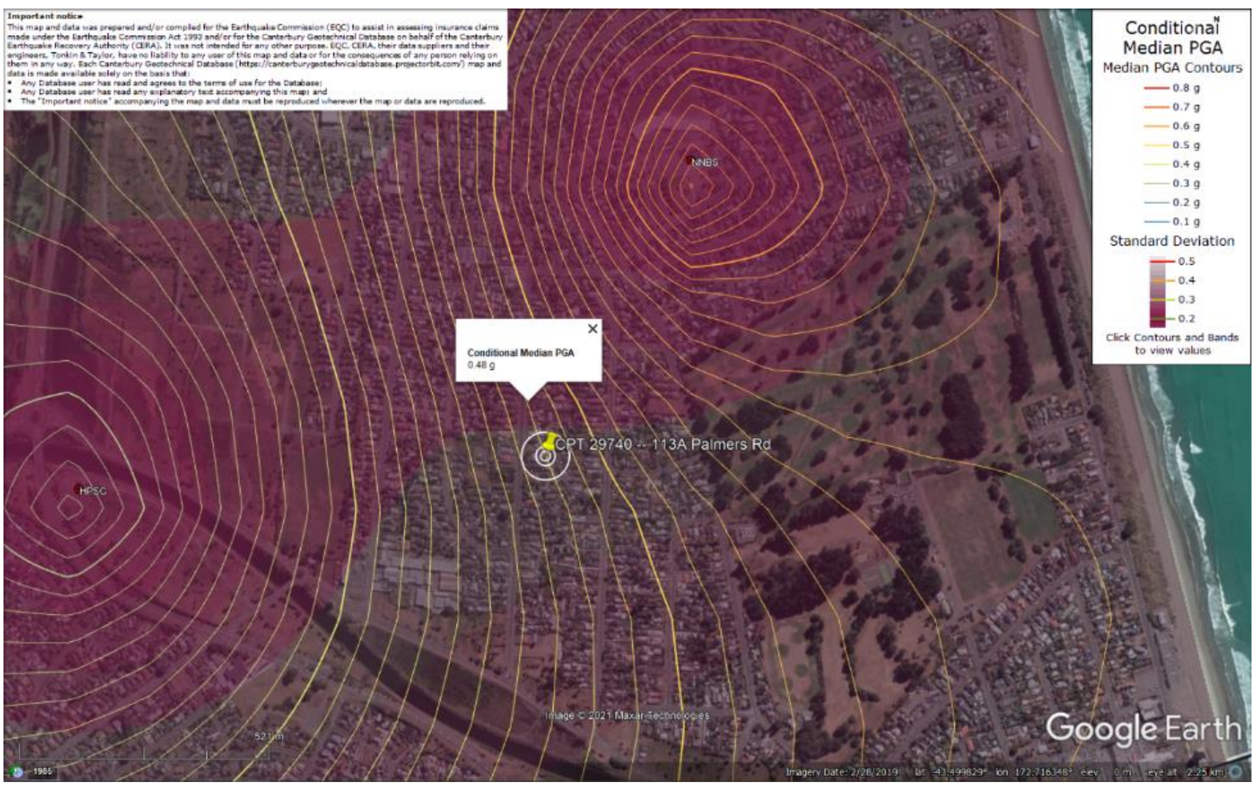

Figure 81: PGA for Feb-11 EQ (st. dev. = 0.275-0.300 ln units).

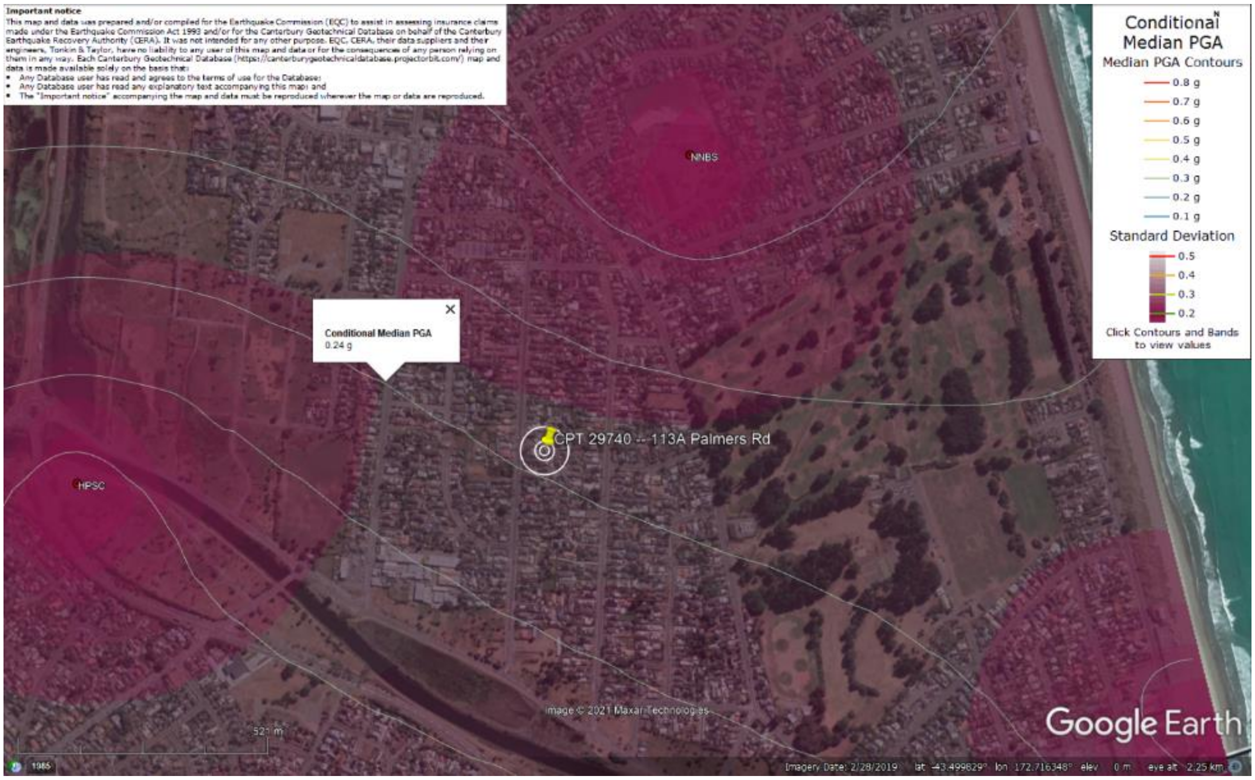

Figure 82: PGA for Jun-11 EQ (st. dev. = 0.275-0.300 ln units).

Figure 83: PGA for Dec-11 EQ (st. dev. = 0.350-0.375 ln units).

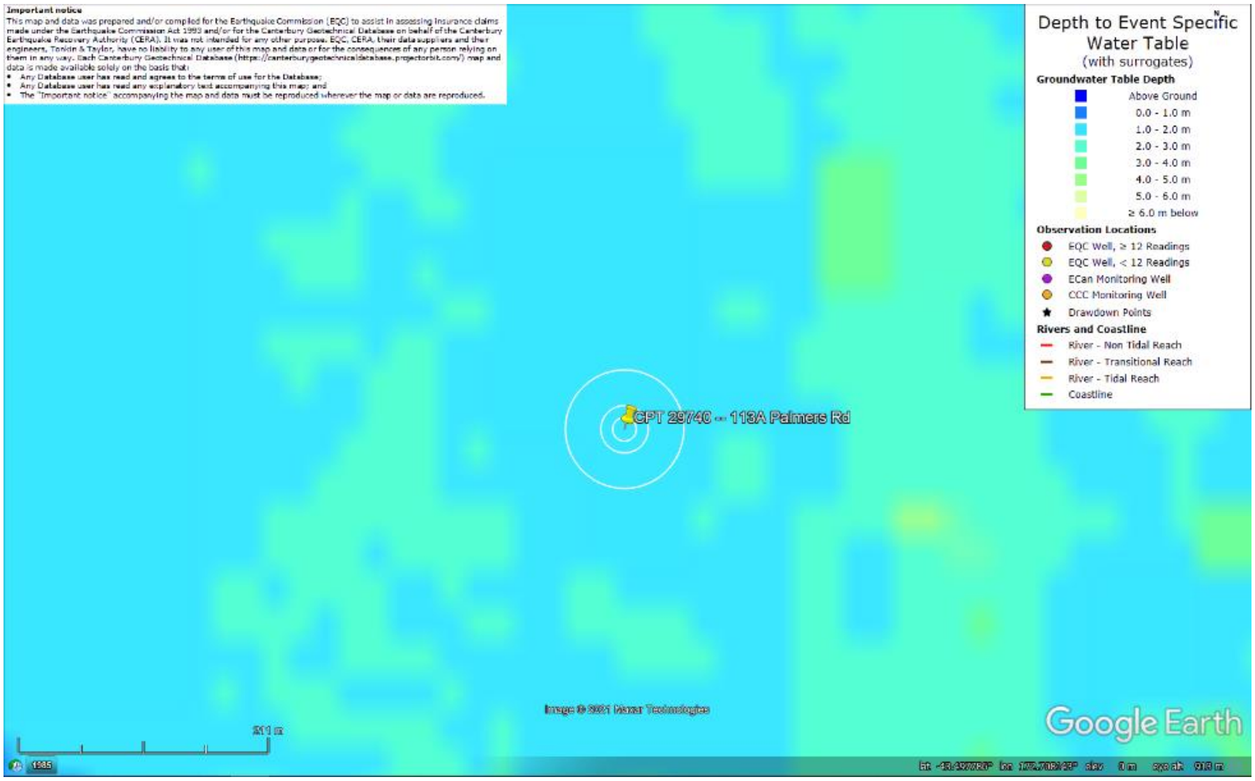

Figure 84: Depth to groundwater table for Sep-10 EQ.

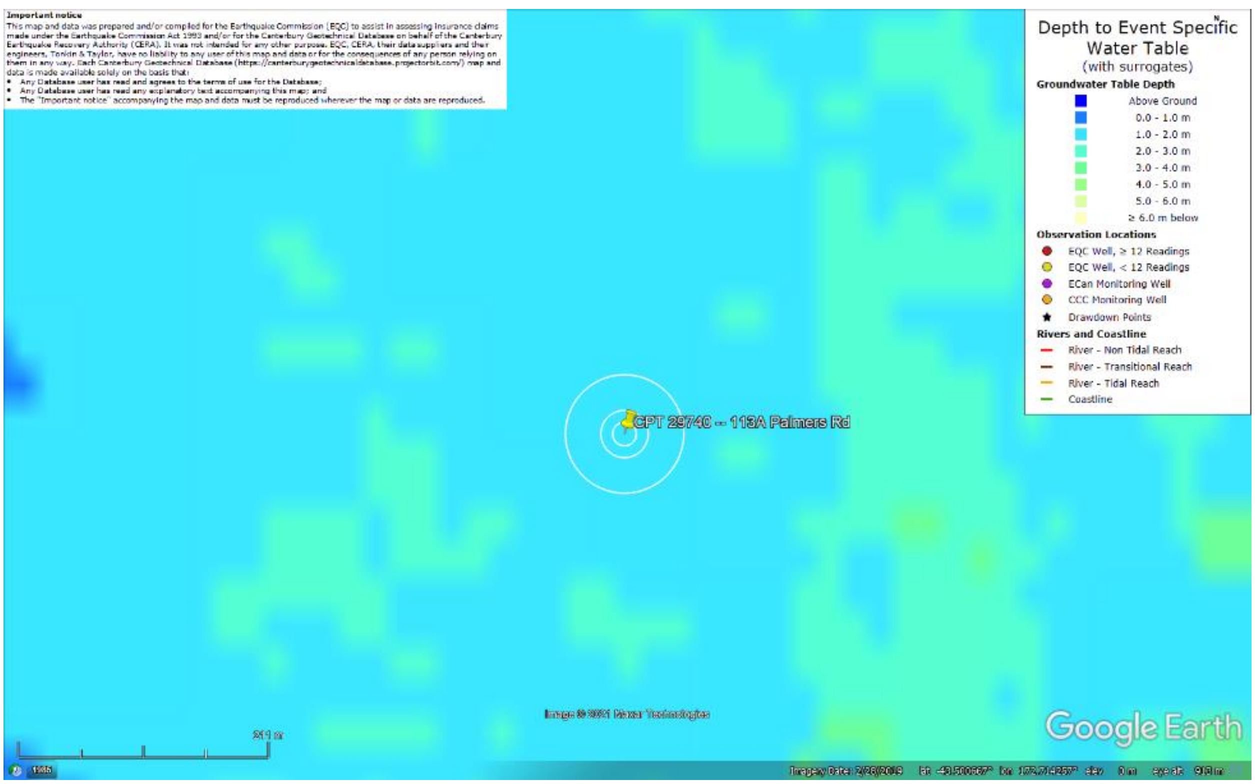

Figure 85: Depth to groundwater table for Feb-11 EQ.

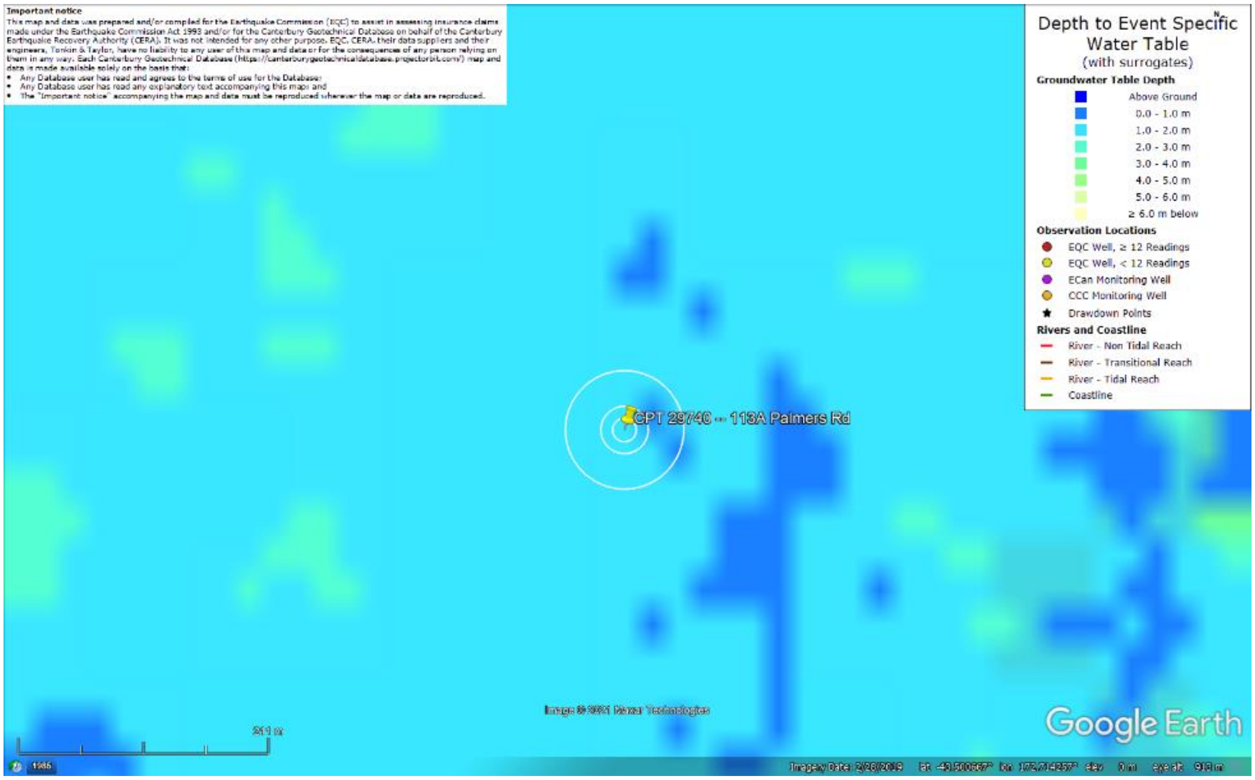

Figure 86: Depth to groundwater table for Jun-11 EQ.

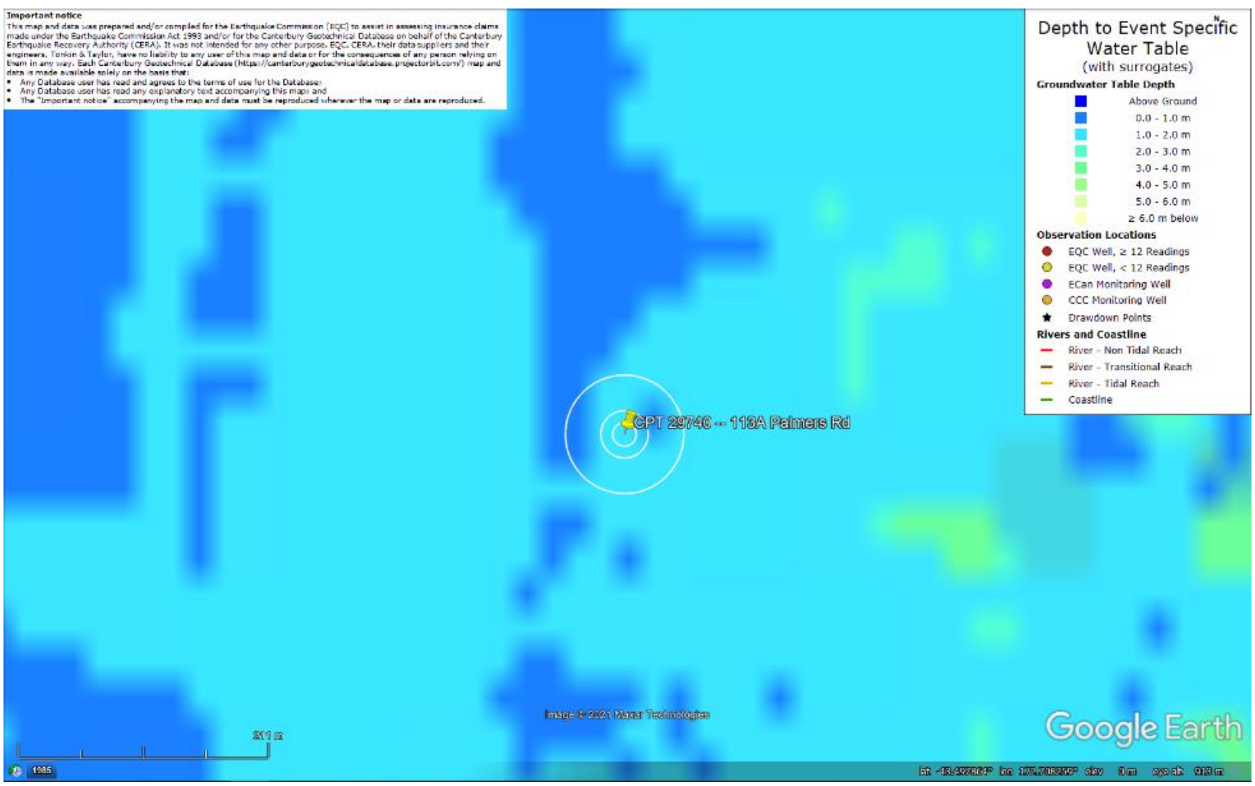

Figure 87: Depth to groundwater table for Dec-11 EQ.

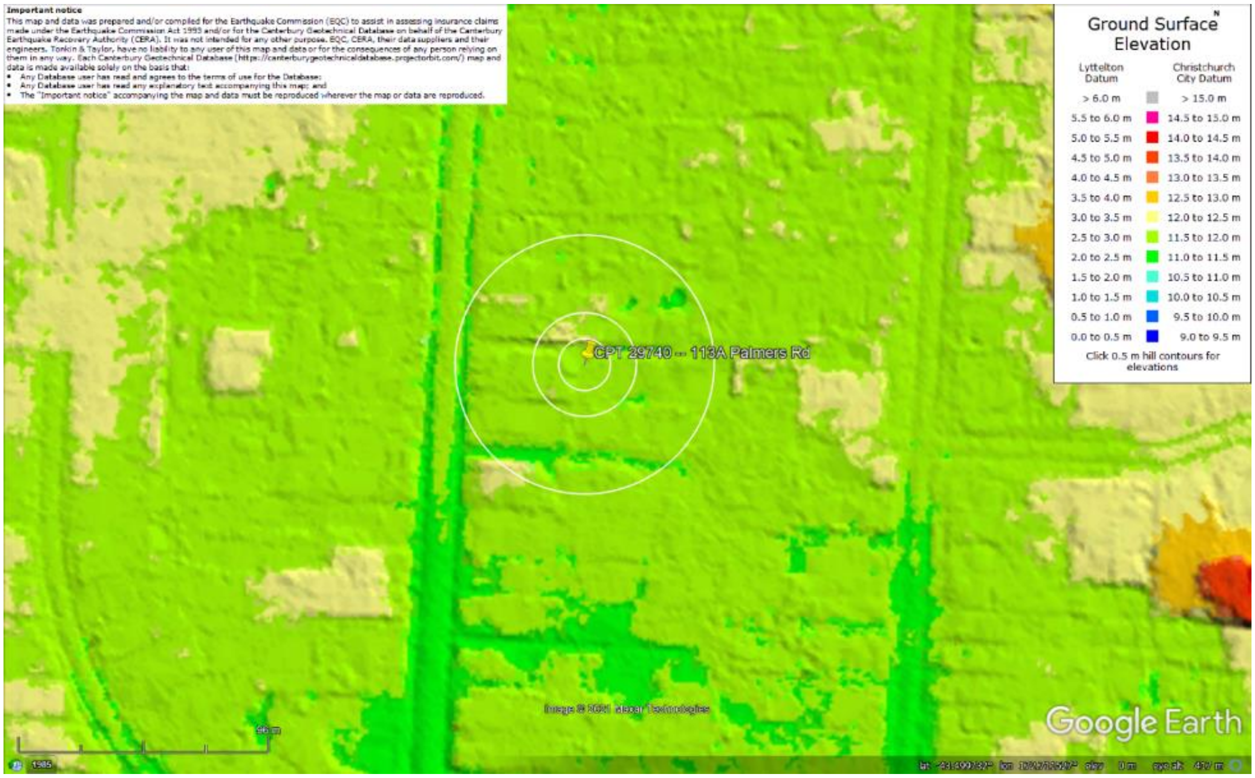

Figure 88: Ground surface elevation according to the Sep-11 LiDAR survey.

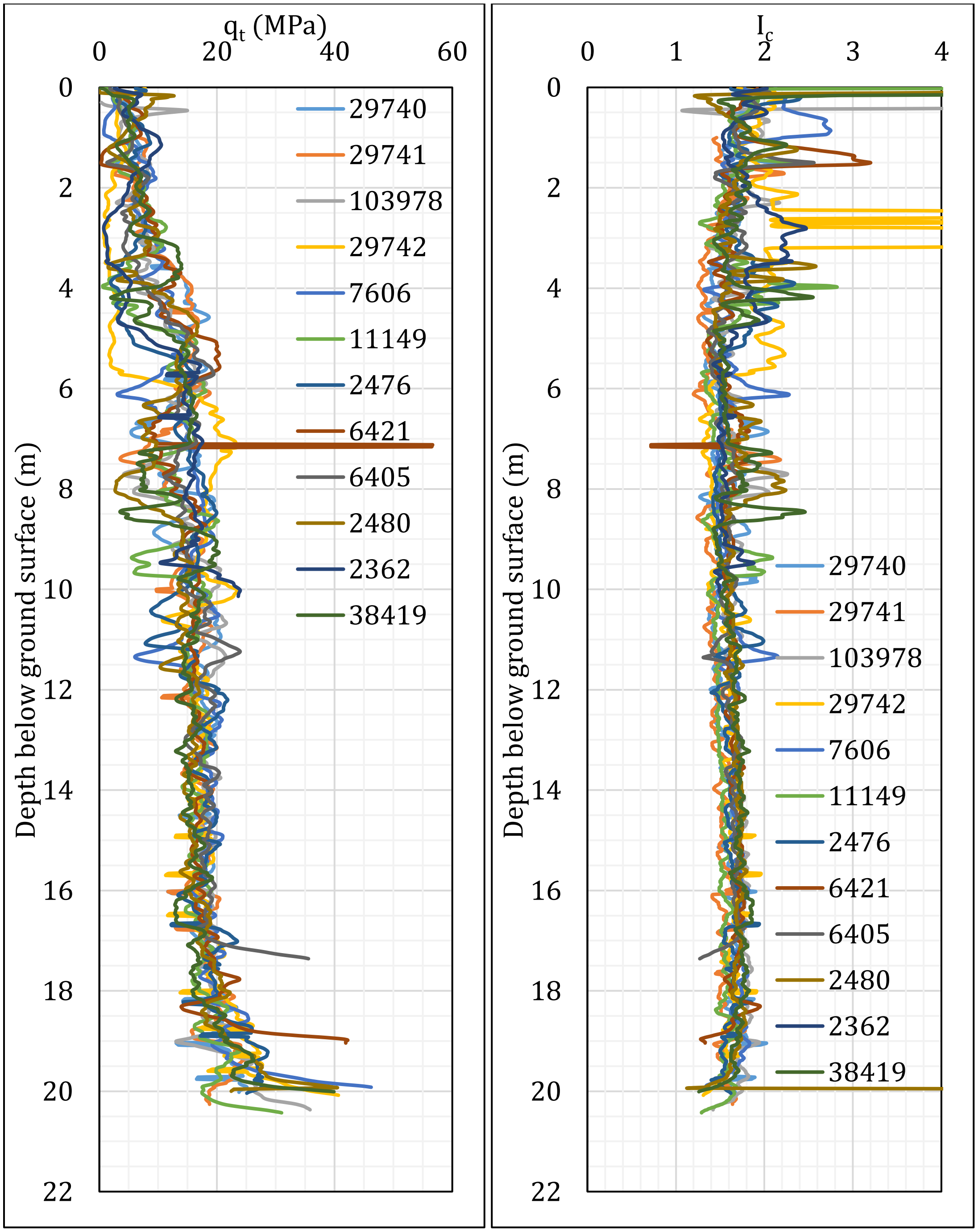

Figure 89: q_t and I_c profiles.

Note 6: The selection of CPTs for the area considered for settlement assessment (Figure 1) is based on the proximity of the CPTs to the considered areas. In accordance with that, the following table shows CPTs that were used for the volumetric settlement analysis in *Cliq v.3.0.3.2*, a CPT soil liquefaction software developed by GeoLogismiki. (The average volumetric settlements were reported in Table 8.)

Table 12: CPT profiles used in volumetric settlement analysis for areas selected for settlement assessment.

CPT ID No.	Patch A	Patch B	Road
29740	✓		
29741	✓		
103978 (89788)			
29742			
7606			
11149			
2476			
6421		✓	
6405			
2480			✓
2362			✓
38419			✓

Note: CPT 29742 was used to compute the volumetric settlement for CPT 2362 for a depth range from 10.1 m to 20 m.

Table 13: CPT-based results.

EQ Event	Parameter	CPT ID 29740	29741	103978	29742	7606	11149	2476	6421
Sep-10	S_{V1D} (mm)	14	17	3	77	6	23	23	3
	LSN	2	3	0	18	1	5	5	1
	LPI	0	1	0	3	0	0	0	0
	LPI_{ish}	0	0	0	1	0	0	0	0
	$D_{FS<1}$ (m)	undet.	7.14	undet.	3.20	undet.	3.69	undet.	undet.
Feb-11	S_{V1D} (mm)	95	107	63	121	59	143	122	94
	LSN	23	23	16	33	14	26	27	20
	LPI	10	11	7	19	7	14	15	8
	LPI_{ish}	9	1	6	10	6	4	13	7
	$D_{FS<1}$ (m)	1.52	1.52	1.90	1.52	2.02	1.51	1.86	1.56
Jun-11	S_{V1D} (mm)	24	29	9	103	14	43	50	9
	LSN	6	6	2	28	3	11	11	3
	LPI	1	1	0	8	0	2	3	0
	LPI_{ish}	0	1	0	7	0	2	1	0
	$D_{FS<1}$ (m)	undet.	6.96	undet.	1.72	undet.	3.39	3.58	undet.
Dec-11	S_{V1D} (mm)	64	75	41	117	43	101	93	47
	LSN	19	19	11	36	11	26	23	13
	LPI	5	6	3	16	4	9	10	3
	LPI_{ish}	5	0	3	14	3	5	5	3
	$D_{FS<1}$ (m)	1.50	1.48	2.16	1.22	2.16	1.21	2.04	1.56

Notes: $D_{FS<1}$ = Depth to the first liquefiable layer (FS_L<1) that is at least 200-mm thick, as determined by the Boulanger and Idriss (2016) liquefaction-triggering procedure (P_L=50%, C_{FC}=0.13, and $I_{c,cutoff}$ =2.6), and exported from *Cliq v.3.0.3.2*; undet. = the specified soil layer was not detected.

Table 13 (continued): CPT-based results.

		CPT ID				
EQ Event	Parameter	6405	2480	2362	38419	$\Delta_{CPT2362}$
Sep-10	S_{V1D} (mm)	11	24	38	12	8
	LSN	4	4	11	2	1
	LPI	0	1	1	0	0
	LPI_{ish}	0	0	0	0	--
	$D_{FS<1}$ (m)	undet.	7.72	2.66	7.66	--
Feb-11	S_{V1D} (mm)	96	159	90	107	18
	LSN	26	31	28	19	1
	LPI	12	18	15	10	0
	LPI_{ish}	12	1	10	7	--
	$D_{FS<1}$ (m)	1.52	1.51	1.60	1.51	--
Jun-11	S_{V1D} (mm)	37	46	61	24	8
	LSN	13	10	18	5	1
	LPI	2	2	4	1	0
	LPI_{ish}	1	1	3	0	--
	$D_{FS<1}$ (m)	2.42	2.39	2.46	2.68	--
Dec-11	S_{V1D} (mm)	71	114	83	63	9
	LSN	26	29	26	15	1
	LPI	8	11	11	5	0
	LPI_{ish}	6	0	9	0	--
	$D_{FS<1}$ (m)	1.34	1.21	1.92	1.24	--

Notes: $D_{FS<1}$ = Depth to the first liquefiable layer (FS_L<1) that is at least 200-mm thick, as determined by the Boulanger and Idriss (2016) liquefaction-triggering procedure (P_L=50%, C_{FC}=0.13, and $I_{c,cutoff}$ =2.6), and exported from *Cliq v.3.0.3.2*; undet. = the specified soil layer was not detected; $\Delta_{CPT2362}$ indicates the amount of SV1D, LSN, and LPI added for CPT 2362 due to the shallow penetration depth.

Note 7: Based on the borehole log (BH 4409, Figure 1), the groundwater table is at a depth of 1.0 m below the ground surface. The soil profile consists of (1) sand with gravel, SW, as fill underlying concrete pavement to a depth of 0.2 m and (2) fine to medium sand, SP, of the Christchurch formation, to a depth of 20 m.

Note 8: The ejecta-induced free-field settlement provided in Table 11 is an areal average settlement due to ejecta, which is based on the total settlement assessment area, A_T (provided in Table 9 and repeated in Table 14). However, the considered area was not always covered completely with ejecta; thus, it is important to provide the localized ejecta-induced settlement, too. The localized settlement due to ejecta is estimated using photographic evidence only as

$$S_{E,P\_localized} = \frac{V_E}{A_E}$$

where V_E is the total volume of ejecta within A_T and A_E is the total coverage area of ejecta within A_T. Please note that the areal ejecta-induced settlement provided in Table 14 as S_{E,P_areal} is the same as $S_{E,P}$ in Table 11, which was estimated as

$$S_{E,P\_areal} = S_{E,P} = \frac{V_E}{A_T}$$

where V_E is the total volume of ejecta within A_T and A_T is the total settlement assessment area.

Table 14a: Areal and localized ejecta-induced settlement estimates for Patch A (10-, 20-, and 50-m buffers) based on photographic evidence.

Earthquake Event	A_T (m^2)	A_E (m^2)	V_E (m^3)	S_{E,P_areal} (mm)	$S_{E,P\_localized}$ (mm)
Sep-10	82.4	0	0	0	0
Feb-11	82.4	78.1	4.0-6.3	65±15	65±15
Jun-11	82.4	82.4	2.2-4.5	40±15	40±15
Dec-11	82.4	82.4	3.5-6.9	65±20	65±20

Notes: S_{E,P_areal} = $S_{E,P}$ reported in Table 11 = areal ejecta-induced settlement; $S_{E,P\_localized}$ = localized ejecta-induced settlement; A_T = total settlement assessment area; V_E = total volume of ejecta within A_T; A_E = total area of ejecta within A_T; The estimates of both areal and localized ejecta-induced settlement are rounded to the nearest 5; Final plus/minus values are also rounded to the nearest 5.

Table 14b: Areal and localized ejecta-induced settlement estimates for Patch C (50-m buffer) based on photographic evidence.

Earthquake Event	A_T (m^2)	A_E (m^2)	V_E (m^3)	S_{E,P_areal} (mm)	$S_{E,P\_localized}$ (mm)
Sep-10	36.2	0	0	0	0
Feb-11	36.2	22.6	2.4-3.6	80±15	130±30
Jun-11	36.2	ND	ND	ND	ND
Dec-11	36.2	ND	ND	ND	ND

Notes: S_{E,P_areal} = $S_{E,P}$ reported in Table 11 = areal ejecta-induced settlement; $S_{E,P\_localized}$ = localized ejecta-induced settlement; A_T = total settlement assessment area; V_E = total volume of ejecta within A_T; A_E = total area of ejecta within A_T; The estimates of both areal and localized ejecta-induced settlement are rounded to the nearest 5; Final plus/minus values are also rounded to the nearest 5; ND = Not determined.

Table 14c: Areal and localized ejecta-induced settlement estimates for Road (50-m buffer) based on photographic evidence.

Earthquake Event	A_T (m^2)	A_E (m^2)	V_E (m^3)	S_{E,P_areal} (mm)	$S_{E,P\_localized}$ (mm)
Sep-10	296	0	0	0	0
Feb-11	296	296	23.7-47.7	120±40	120±40
Jun-11	296	296	11.7-29.3	70±30	70±30
Dec-11	289	289	14.2-28.4	75±25	75±25

Notes: S_{E,P_areal} = $S_{E,P}$ reported in Table 11 = areal ejecta-induced settlement; $S_{E,P\_localized}$ = localized ejecta-induced settlement; A_T = total settlement assessment area; V_E = total volume of ejecta within A_T; A_E = total area of ejecta within A_T; The estimates of both areal and localized ejecta-induced settlement are rounded to the nearest 5; Final plus/minus values are also rounded to the nearest 5.

Summary 2:

- **The best estimate of the localized ejecta-induced free-field ground settlement at the 113A Palmers Rd site for the SEP 2010, FEB 2011, JUN 2011, and DEC 2011 earthquake is 0 mm, 65±15 mm, 40±15 mm, and 65±20 mm, respectively.**
- **The best estimate of the localized ejecta-induced free-field settlement of the road at the 113A Palmers Rd site for the SEP 2010, FEB 2011, JUN 2011, and DEC 2011 earthquake is 0 mm, 120±40 mm, 70±30 mm, and 75±25 mm, respectively.**